THESIS

INFLAMMATORY EFFECTS OF COOK STOVE EMISSIONS ON CULTURED HUMAN BRONCHIAL EPITHELIAL CELLS

Submitted by

Brie Hawley

Department of Environmental and Radiological Health Sciences

In partial fulfillment of the requirements

For the Degree of Master of Science

Colorado State University

Fort Collins, Colorado

Summer 2010

COLORADO STATE UNIVERSITY

June 17, 2010

WE HEREBY RECOMMEND THAT THE THESIS PREPARED UNDER OUR SUPERVISION BY BRIE HAWLEY ENTITLED INFLAMMATORY EFFECTS OF COOK STOVE EMISSIONS ON CULTURED HUMAN BRONCHIAL EPITHELIAL CELLS BE ACCEPTED AS FULFILLING IN PART REQUIREMENTS FOR THE DEGREE OF MASTER OF SCIENCE.

Committee on Graduate Work

_____

Stephen Reynolds

_____

Bryan Willson

_____

Advisor: John Volckens

_____

Department Head: Jac Nickoloff

ABSTRACT OF THESIS

INFLAMMATORY EFFECTS OF COOK STOVE EMISSIONS ON CULTURED HUMAN BRONCHIAL EPITHELIAL CELLS

Approximately half the world's population uses biomass as a fuel for cooking and heating. This form of combustion is typically achieved by burning wood in a primitive indoor cook stove. Human exposure to combustion byproducts emitted from these 'traditional' stoves is an important global health concern. Such exposures cause an estimated two million premature deaths each year and have been associated with increased incidence of pulmonary disease, eyesight degradation, cancer, and adverse pregnancy outcomes.[1] Many types of 'improved cook stoves' have been developed over the past few decades to address this concern. The aim of this research was to compare the effects of traditional and improved cook stove emissions on normal human bronchial epithelial cells exposed to a single biomass combustion event. We used a direct, aerosol-to-cell deposition system to expose cell cultures to cook stove emissions. We then quantified the relative expression of three different mRNA transcripts associated with a cellular inflammation at 1 and 24 hours following exposure. We hypothesized that cultured human bronchial epithelial cells exposed to wood smoke from an improved cook stove would produce lower levels of inflammatory transcripts as compared to cells exposed to emissions from a traditional stove. Wood smoke was generated from three stove types: an energy efficient model designed and distributed by Envirofit International, an energy efficient model designed and distributed by Philips Inc., and a traditional three

stone fire. The emissions from each cook stove were substantially different, with the three stone fire having the highest emissions of particle number, particle size, and particle mass. Cellular expression of inflammatory genes was also significantly higher in exposed vs. control cells, with the three stone fire having the greatest effect. These results provide preliminary evidence that improved cook stoves have the potential to improve human health.

Brie Hawley
Department of Environmental and Radiological Health Sciences
Colorado State University
Fort Collins, CO 80523
Summer 2010

TABLE OF CONTENTS

LIST OF FIGURES

LIST OF TABLES

LIST OF ALL ABBREVIATIONS, ACRONYMS, AND SYMBOLS

A_{growth}	area of cellular growth, in centimeters squared
ALI	air-liquid interface
ALRI	acute lower respiratory tract infection
ANOVA	analysis of variance
BEBM	Bronchial Epithelial Basal Medium
BEGM	Bronchial Epithelial Growth Medium
C_6H_6	benzene
C_{down}	particle count downstream of electrostatic aerosol in vitro exposure system
CH_4	methane gas
C.I.	95% confidence interval
cm	centimeter
cm^3	cubic centimeters
CMD	count median diameter
CO	carbon monoxide
CO_2	carbon dioxide
C_{off}	particle counts per cubic centimeter of air exiting the electrostatic aerosol in vitro exposure system with the repeller off
C_{on}	particle counts per cubic centimeter of air exiting the electrostatic aerosol in vitro exposure system with the repeller on
COPD	chronic obstructive pulmonary disease
COX-2	cyclooxygenase-2
CPC	condensation particle counter
C_{up}	particle counts upstream of electrostatic aerosol in vitro exposure system
D_i	estimated particle deposition on cell culture well, expressed as a fraction
DMEM-H	Dulbecco's Modified Eagle Medium, high glucose
d_p	diameter of particle
E	collection efficiency of the electrostatic aerosol exposure in vitro system, as a percent
EAVES	electrostatic aerosol in vitro exposure system
EECL	Engines and Energy Conversion Laboratory
EPA	Environmental Protection Agency
$\sum F$	sum of all fluorescence measured in electrostatic aerosol in vitro exposure chamber
F_i	fluorescence measured in each well location of cell exposure plate
GAPDH	glyceraldehyde 3-phosphate dehydrogenase
GCS	glutamylcysteine synthetase
GM-CSF	granulocyte-macrophage colony stimulating factor
H_2	hydrogen gas
HEPA	high efficiency particulate air
HIV	human immunodeficiency virus
HOX-1	hemeoxygenase-1
HSP-27	heat-shock protein 27
HSP-70	heat-shock protein 70
HSP-90	heat shock protein 90
ICAM-1	intercellular adhesion molecule-1
IL-1	interleukin-1

IL-6	interleukin-6
IL-8	interleukin-8
kg	kilograms
kV	kilovolts
ℓ	fractional particle losses in electrostatic aerosol in vitro exposure system
L	liters
LDH	lactate dehydrogenase
%LDH	percent lactate dehydrogenase released in cell exudate
$LDH_{exposed}$	estimated lactate dehydrogenase released in cell exudate
LDH_{max}	maximum amount of lactate dehydrogenase released in cell exudate
m	meters
m^3	cubic meters
mm	millimeters
min	minutes
MIP-1	macrophage inflammatory protein 1
mRNA	messenger ribonucleic acid
MnSOD	manganese superoxide dismutase
NHBE	normal human bronchial epithelial
nm	nanometers
nM	nanomolar
NO	nitrogen oxide
NO_x	nitrogen oxides
NO_2	nitrogen dioxide
OSHA	occupational health and safety administration
PAHs	polycyclic aromatic hydrocarbons
PM	particulate matter
PM_{10}	particulate matter with an aerodynamic diameter smaller than 10 micrometers
PM_{10}	mass of PM_{10} collected upon Teflon filter
$[PM_{10}]$	estimated concentration of PM_{10} mass produced by a cook stove
PM_{dep}	estimated PM_{10} mass delivered to cells per unit of cellular growth area
ppb	parts per billion
ppm	parts per million
Q_E	air flow through the electrostatic aerosol in vitro exposure system in cubic meters per minute
RA	retinoic acid
RH	relative humidity
ROS	reactive oxygen species
RT PCR	reverse transcriptase polymerase chain reaction
SMPS	sequential mobility particle sizer
t	duration of cellular exposure in minutes
µA	microamperes
µg	micrograms
µm	micrometers
ultrafine PM	particulate matter with a diameter smaller than 100 nm
V_{total}	total volume of air passed over a Teflon filter during a cook stove test, in cubic meters
WHO	World Health Organization

1. Introduction

1.1 Global, Residential Biomass Combustion

Biomass combustion is a global phenomenon, producing both ambient and indoor air pollution throughout the entire world. Outdoors, this form of anthropogenic combustion is dominated by slash and burn techniques, whereby forests are cleared and burned for the temporary creation of fertile farmland for crop or livestock production. The burning of forests increases the atmospheric burden from particulate matter, a public health hazard, and CO_2, the primary greenhouse gas associated with global climate change. Biomass is burned indoors for the domestic production of light and heat. Indoor biomass combustion promotes survival and comfort through the heating of homes and is also relied upon as a cooking practice to nourish and sustain humans. The biomass fuel used for heating and cooking is typically burned indoors in an open fire, or in a simple cook stove.[1]

1.2. Indoor Combustion of Biomass Fuels

Approximately half of the world's population relies on coal and other biomass fuels (wood, dung, and crop residues) to conduct daily cooking activities and to heat their homes[1]. This type of combustion accounts for approximately one-tenth of human energy use on the planet.[2, 3] Wood accounts for 50-60% of the biomass fuel used for domestic combustion.[4] However, the combustion of wood in open fires or in simple cook stoves is very inefficient, which leads to several domestic, environmental, and public health concerns.

The domestic concern is significant for individuals who rely on wood for cooking and heating, as the task of procuring firewood can involve long, arduous treks in search of a diminishing resource.[2] Environmental concerns include the depletion of forests, a limited resource, in addition to the release of CO_2, a greenhouse gas, into the atmosphere. Between 1950 and 1990, the amount of wood used annually for fuel increased from 1500 to 3500 million cubic meters, and this rate of consumption is expected to increase.[5] The public health concern is perhaps most significant, as half the world's population is currently exposed to emissions from indoor biomass combustion.[1] Exposure to indoor air pollutants emitted during biomass combustion is a significant contributor to human morbidity and mortality in developing countries. A recent assessment of the global burden of disease conducted by the World Health Organization found that, of the top thirty causes of death worldwide, lower respiratory infections ranked fourth, chronic obstructive pulmonary disease (COPD) ranked sixth, tuberculosis (TB) – HIV seropositive excluded – ranked seventh, and tracheal, bronchial, and lung cancers ranked tenth.[6] Chronic exposure to wood burning emissions has been implicated as a risk factor for the development of all of the aforementioned diseases.[6,7]

1.3. The Need for an Improved Cook Stove

There is a need for the development and distribution of fuel efficient cook stoves from both an environmental and human health perspective. Reducing a stove's fuel consumption would decrease deforestation and the time and energy spent by individuals gathering fuel. A more fuel efficient stove would also help mitigate indoor air pollution by reducing emissions during combustion. Consequently, there has been a global effort to develop and distribute improved cook stoves. Between 1977 and 1985 approximately 43

million improved stoves were distributed in developing countries.[5] There are several hundred improved cook stove projects ongoing worldwide.[8]

1.4. Air Pollution from Biomass Fuel Combustion

Emissions from biomass combustion consist of a complex mixture of gases and particulate matter (PM). The blackened walls shown in Figure 1 provide evidence of the particulate matter burden from biomass combustion indoors.

Figure 1. **A home in India with walls blackened by PM from biomass combustion**[9]

Ideally, biomass combustion would convert 100% of the hydrocarbon (biomass) fuel into heat, light, carbon dioxide, and water. However, combustion is rarely ideal and often results in the release of combustion byproducts, including gases such as carbon monoxide (CO), nitrogen oxides (NO_x), and a wide variety of volatile and semi-volatile organic

carbon species, as well as fine particulate matter.[4] The extent and relative proportions of these emissions can vary with fuel type, stove design, temperature, altitude, humidity, local ventilation, and cooking technique.[2]

1.4.3. Carbon monoxide (CO)

Carbon monoxide is a colorless, odorless gas formed during incomplete combustion; this pollutant is often used to characterize the completeness of combustion, in conjunction with carbon dioxide (CO_2), since these two species constitute the vast majority of biomass combustion emissions, by mass.[10]

Acute CO exposure causes headache, flushing, nausea, vertigo, weakness, irritability, unconsciousness, and pain in the chest and legs in persons with pre-existing heart disease or atherosclerosis.[11]

Chronic exposure to CO at levels above 35 ppm may cause more persistent symptoms, such as anorexia, headache, lassitude, dizziness, and ataxia.[11] Infants, children, and the elderly are more susceptible to the effects of CO. In the U.S., ambient CO concentrations are regulated by the U.S. Environmental Protection Agency at 8.7 and 35 ppm for 8-hr and 1-hr time-weighted averages, respectively.[12] The U.S. Occupational Safety and Health Association mandates that indoor concentrations in the workplace not exceed 200 ppm. Concentrations above 1200 ppm are immediately dangerous to life and health.[11]

Peak concentrations in homes with wood burning fires or traditional stoves approach or exceed the EPA's one hour standard of 35 ppm for carbon monoxide. Several studies have investigated indoor air concentrations of CO in homes with indoor biomass combustion. In studies that measured carbon monoxide over the course of a day, average levels ranged from 8.7-52 ppm[13] to 37 ± 27 ppm, [14] with peak levels occurring during

cooking events.

These studies conducted area monitoring of indoor air pollutants, which is an indirect means estimating personal exposure. The measurement of carboxyhaemoglobin levels is a more direct assessment of personal CO exposure. Carboxyhaemoglobin is formed when carbon monoxide is inhaled, as carbon monoxide binds to hemoglobin with an affinity 230 times greater than oxygen.[15] One study found that non-smoking women between the ages of 25 and 30 years exposed to smoke from biomass fuels had carboxyhaemoglobin concentrations of 15.74% (± 0.83%) while unexposed women had concentrations of 3.53% (± 0.33%).[16,17] The level of carbon monoxide in the blood of women exposed to biomass combustion emissions was 4-5 times greater than the reference group, providing evidence that biomass burning is a significant contributor to carbon monoxide exposure.[16,17]

1.4.3. Nitrogen oxides (NO_x)

Nitrogen oxides include nitrogen dioxide, nitric oxide, and nitrous oxide. NO_x is formed from the presence of nitrogen in the air used for combustion. Acute Exposure to NO_2 causes irritation to the eyes, nose, throat and respiratory tract. Nitrogen dioxide exposure is also associated with pulmonary edema and diffuse lung injury.[18] Chronic exposure to NO_2 is associated with incidence of acute or chronic bronchitis and an overall increased risk of respiratory tract infections, especially in young children.[19] Nitrogen dioxide has been shown to affect the mucociliary apparatus and has also been shown to affect humoral and cellular defenses, thereby increasing susceptibility to infections.[19] The U.S. EPA mandates that nitrogen dioxide not exceed 0.057 ppm over the course of 24 hours,[18] whereas the WHO suggests that nitrogen dioxide not exceed 0.021 ppm when

averaged over the course of a year.[20]

The indoor concentration of nitrogen dioxide in wood-burning homes has not been studied extensively, but measured levels have been appreciable, nonetheless. Two studies conducted in Ethiopia found ambient levels of NO_2 ranging from 0.034-0.068 ppm[21] when monitored over a twenty-four hour period, with averages of 0.051 (± 0.047) ppm and 0.04 (± 0.001) ppm.[22] Since wood burning is relied upon daily, the exceedance of the WHO's annual exposure limit is of concern.

1.4.3. Volatile and Semi-Volatile Organic Carbon Species

The number of volatile and semi-volatile organic carbon species found in wood burning emissions is extensive. Aromatics like benzene, aldehydes like formaldehyde and acrolein, and polycyclic aromatic hydrocarbons like naphthalene, fluorene, phenanthrene, and benzo(a)pyrene, are a few of the hazardous volatile and semi-volatile organic carbon species that have been found in homes relying on biomass combustion.

1.4.3.1. Aromatics (C_xH_x)

Benzene (C_6H_6) is the most studied aromatic compound in homes relying on wood burning for fuel. Short-term exposure to high levels of benzene can cause drowsiness, dizziness, unconsciousness, and even death.[23] Long-term exposure to low levels of benzene has been associated with the development of blood and bleeding disorders, disruption of immune responses, and leukemia.[23] Benzene is classified as a Group A, human carcinogen.[23] The California EPA has limited safe exposure to 19 ppb due to benzene's hematological effects.[23] The few studies that have measured indoor levels of benzene in wood burning homes reported concentrations ranging from 9-260 ppb.[24, 25] This range reflects the dynamic variation in indoor emission/ventilation rates; a level of

260 ppb is well over ten times the safe exposure limit.

1.4.3.2. Aldehydes (O=CH-R)

Acrolein (C_3H_4O) and formaldehyde (CH_2O) are two aldehydes measured in appreciable levels in wood smoke emissions. In one study, measured concentrations of aldehydes (the majority being formaldehyde and acrolein) in wood burning homes ranged from 0.3-1.0 ppm.[26] These levels have been associated with irritation of the upper airways, headaches and other central nervous system dysfunction, asthma exacerbation, and possibly cancer.[27]

Formaldehyde concentrations have been well studied in homes that burn wood. The Agency for Toxic Substances and Diseases Registry established a minimal risk for non-cancer respiratory symptoms associated with formaldehyde levels above 0.003 ppm, while exposure to levels higher than 0.008 ppm is associated with increased risk for nasal or leukemia cancers.[27] Research that selectively monitored formaldehyde in the indoor air of village houses found levels ranging from an average of 0.1 ppm over an entire week, to 2 ppm during cooking conditions, well above levels that increase the risk of disease.[28, 29]

1.4.3. Polycyclic Aromatic Hydrocarbons (PAHs)

Incomplete combustion produces numerous polycyclic aromatic hydrocarbons whose vapor pressures allow them to distribute in both gas and particulate phases. In a study of PAHs in wood burning homes, four volatile PAHs were found in appreciable concentrations: naphthalene, fluorene, phenanthrene and acenaphthene. Naphthalene represented 60-70% of the total PAH measured in the ambient air, with a mean concentration of 5.5 (± 4.5) ppm.[14] Levels of naphthalene above 1.7 ppm have been

associated with hyperplasia of the respiratory epithelium and nasal olfactory metaplasia.[30] Chronic exposure to naphthalene is associated with increased risk for cataracts, retinal damage, and inflammation of the nasal and lung epithelia.[30]

1.4.3. Particulate Matter ($d_p < 2.5$ μm)

Wood burning aerosols are predominantly smaller than 2.5 μm in diameter, as the majority of particulate matter from combustion is generated within the nucleation and accumulation size modes (0.001 μm < d_p < 1.2 μm).[31] Indoor PM concentrations vary with different wood burning practices and different ventilation inherent in the homes sampled. Typical levels in households with open burning range from 100 to 2000 μg/m^3, with peaks during cooking reaching levels five to ten times higher.[4]

Particles smaller than 2.5 μm are capable of depositing in the distal, alveolar region of the lungs.[32] Particles depositing in the alveolar region have longer residence times due to limited clearance and may be retained for decades in this region of the lung. Thus, the duration of exposure for pulmonary cells can extend well beyond the initial inhalation event.[32]

Ultrafine PM, defined as particles with a diameter less than 0.1 μm, can deposit within and pass through the alveoli. Ultrafine particles can gain access to the cardiovascular system, where they may deposit along the walls of blood vessels. Ultrafine PM exposure has been implicated in the development of arrhythmic, ischemic, and pro-thrombotic cardiovascular effects.[33]

1.4.3. Regional and Cultural Variations in Exposure

The intensity and duration of human exposure to cook stove emissions can vary greatly with regional and cultural practices. Region can affect both the intensity and

duration of exposure. For example, colder climates typically necessitate continuous burning of fuels to heat homes that are more tightly sealed, having less ventilation than homes in warmer climes.[7, 34] In most cultures, women are the predominant stove users, leading to greater exposures for females worldwide.[7, 34] Women are also the primary care providers for children, which can lead to increased exposures for children who are in close proximity to their mothers.[7] Further differences exist in the duration and intensity of cooking events. Some cultures exhibit cooking practices that lead to a continuous simmer (i.e., continuous emissions) while other cultures tend to cook only for distinct periods, leading to di- and triurnal exposure patterns associated with each meal.

1.5. Health Effects of Exposure to Biomass Combustion Emissions

A meta-analysis of current epidemiological evidence found that adult women using solid household fuels are 3.2 times (95% C.I.: 2.3-4.8) more likely to suffer from chronic obstructive pulmonary disease, 1.9 times (95% C.I.: 1.1-3.5) more likely to suffer from lung cancer, 1.3-1.6 times more likely to suffer from blindness due to cataracts, and 1.5-3.0 times more likely to suffer from Tuberculosis than adult women living in households burning cleaner fuels.[4] The relative risks for men living in homes that burn biomass are lower than for women, which is not surprising since women are typically the principal stove user in the home. However, the relative risk for male chronic obstructive pulmonary disease (1.8, 95% C.I.: 1.0,3.2) and lung cancer (1.5, 95% C.I.: 1.0-2.5) was still elevated for men living in homes with biomass burning compared to men exposed to cleaner-burning fuels.[4] Other morbidities include cor pulmonale, an enlargement of the heart that is associated with chronic obstructive pulmonary disease. Cor pulmonale has been increasingly observed in nonsmoking women whose chief risk factor is exposure to

wood burning smoke.[35]

In children younger than five years of age, acute lower respiratory infections (ALRI) are reported as the second-most common cause of death, behind neonatal causes (infection, pre-term birth, and birth asphyxia).[36] Exposure to emissions from biomass burning is estimated to be responsible for 1 million premature ALRI deaths in children each year. Acute lower respiratory infections in young children are thought to be the largest single impact of biomass exposure. Most of their exposure occurs while under the care of their mothers.[4] Since ALRIs affect children more severely, they cause more lost life-years than any other disease.[37] A review of the studies focusing on children in homes where biomass is burned found that children had approximately twice the ALRI rate of those living in households with cleaner fuels.[36, 38] Smith (2006) found that the introduction of a well-operating chimney stove caused the greatest reduction in the most serious forms of ALRI.[39]

Adverse pregnancy outcomes have also been linked to biomass combustion exposures, though the evidence is not as strong. Carbon monoxide exposure is associated with adverse pregnancy outcomes since it displaces the supply of oxygen to the developing fetus.[4]

1.5.3. Human Inhalational Exposure Studies

Human inhalational exposure studies that assess the physiological response after exposure to wood smoke are few, but Barregard et al. from Sweden have conducted several studies with interesting findings. In 2006 and 2008, Barregard et al. reported increases in serum levels of Clara cell protein and alveolar nitric oxide, along with Amyloid A and C-reactive proteins in human sera following acute wood smoke exposure,

providing evidence that wood smoke leads to both pulmonary and systemic inflammation.[40, 41] These findings suggest that exposure to wood smoke results in oxidative stress and a local airway and systemic inflammatory response in the human body.

1.5.3. Cellular Pathology Associated with Biomass Combustion PM

Although epidemiological and inhalational studies have shown a relationship between PM levels and morbidity and mortality amongst exposed populations and individuals, the molecular pathways by which combustion-derived PM exerts toxic effects on the cardiopulmonary system are still being elucidated.

Many studies have shown that exposure to ambient PM is associated with increased levels of reactive oxygen species (ROS) in the lungs and heart in vivo.[42] Wood smoke has been shown to be a source of free radicals that stimulate the formation of ROS within the cell.[43, 44] Both transition metals and quinones are present within PM, and these molecules are capable of producing ROS though Fenton-like reactions in solution.[45] Cellular accumulation of ROS can result in the increased production of protective enzymes, such as: superoxide dismutase, glutathione reductase, glutathione peroxidase, and catalase.[46] These enzymes work to reduce oxidative stress within the cell.

However, PM can also inhibit the function of these protective enzymes, thereby decreasing the cell's ability to alleviate oxidative stress.[47] Transition metals within the PM may inhibit enzymes that protect against oxidative stress.[47] Such inhibition may be detrimental, as ROS have been associated with alveolar damage, macrophage stimulation, inflammation, and fibrosis in the lung.[48]

Wood combustion PM also causes DNA damage in human monocytic (macrophage

pre-cursors) and epithelial cell lines.[49, 50, 51] Such damage is also attributed to free radical formation and oxidative stress. Wood smoke also has the potential to produce mutations in the DNA, which are largely associated with the polycyclic aromatic hydrocarbon content of the PM.[47] For example, benzo(a)pyrene, which is present in wood smoke, has been implicated in DNA adduct formation and is listed as a probable human carcinogen by the International Agency for the Research on Cancer.[52] Polycyclic aromatic hydrocarbons in combustion emissions have long been studied for their carcinogenic potential, having first been identified as increasing the risk for cancer in London's chimney sweepers in 1775.[29]

The increased burden from inhaled oxidants in wood smoke and the associated reactive oxygen species produced in lung tissue is known to initiate an inflammatory response in the respiratory epithelium. The inflammatory response often includes the activation of resident macrophages and the recruitment of neutrophils, eosinophils, monocytes, and lymphocytes.[53] The recruitment and activation of these immune cells often confounds the damage caused by the inhaled oxidants, by producing secondary, metabolic reactive oxygen species like superoxide, hydrogen peroxide, and hydroxyl radicals.[53] Cellular production of inflammatory coordinators like TNF-α increase when macrophage, alveolar, and bronchial epithelial cells are exposed to inhalable oxidants. TNF-α stimulates airway epithelial cells to transcribe genes for pro-inflammatory cytokines and chemokines like IL-8, IL-1, inducible NO synthase, COX-2, ICAM-1, IL-6, MIP-1, GM-CSF, stress response genes like HSP-27, 70, 90, HOX-1, and antioxidant enzymes like glutamylcysteine synthetase, GCS, MnSOD, and thioredoxin.[53] The induction of any one of these genes is associated with inflammation of the human lung.

1.6. Improved Stove Hypothesis

With the potential to improve the lives of close to half the world's population, an improved cook stove appeals to many groups seeking to alleviate the social, economic, and health burdens from inefficient biomass combustion. An "improved" cook stove operates with increased combustion efficiency, which, theoretically, results in increased fuel efficiency and reduced emissions. Greater fuel efficiency means that less time and money would be spent procuring wood, a limited resource. More time could be devoted to other individual/familial needs, making the practice of biomass burning more sustainable. Improved combustion efficiency should also lead to fewer emissions and fewer harmful by-products from incomplete combustion.

However, quantifying the global impact from an improved cook stove is a complex and multifaceted process. The more focused objective of this research was to evaluate acute inflammation in cultures of normal human bronchial epithelial cells after exposure to wood combustion emissions from traditional and improved cook stoves. We hypothesize that cells exposed to improved cook stove emissions will produce less inflammatory markers compared to cells exposed to emissions from a traditional, three-stone fire.

1.7. Modeling PM Health Effects In Vitro

1.7.1. In Vitro Exposure Models

Many studies rely upon animal models to understand the respiratory health effects of combustion emissions. However, given the inherent differences between humans and the widely used rodent model (rodents are obligate nasal breathers), animal studies are limited in their ability to model human inhalational exposures. Animal studies are also

costly in terms of space, energy, and waste. Therefore, researchers have also turned to in vitro models of the respiratory and cardiovascular epithelia, using both human and animal cell cultures. The process of culturing and exposing lung cells in vitro offers a cost-effective means of assessing the physiological response of the human lung to inhaled toxicants. However, traditional models of the human lung in vitro are limited in their physiological relevance.

1.7.2. Traditional In Vitro Exposure Techniques

Traditional models of lung exposure to PM are severely limited in their physiological relevance. The most widely used technique for in vitro lung cell exposures currently relies upon growing cells submerged in growth media and exposing them to PM-extracts or a resuspended PM hydrosol. The particle suspension is then dispensed upon the submerged cells. Particle extraction may involve harsh solvents, is rarely 100% efficient, and introduces biases due to particle agglomeration, dissolution, or reaction. Delivery of particles suspended in liquid to respiratory tract cells also makes it difficult to compare the dose of particles on the cells to the particle dose seen by cells during inhalation, sometimes resulting in doses delivered in vitro that may be orders of magnitude larger than those studied in vivo.[54] The physiological relevance of this technique is debatable, as it grossly oversimplifies what occurs in the human lungs during actual exposure.

1.7.3. Novel Technique: Air-liquid Interface Exposure

The advent of air-liquid interface cultures, whereby cells are grown on a semi-permeable membrane above a reservoir of growth media, substantially improved our ability to model the human lung in vitro.[55] The ability to culture primary human airway epithelial cells on a semi-permeable membrane offers two main advantages: (1) the cells

undergo differentiation to resemble the cellular structures found in vivo and (2) the air liquid interface allows for direct deposition of PM onto the apical surface of the cells.[56]

The culture of normal human bronchial epithelial (NHBE) cells at an air liquid interface with an appropriate growth medium has been shown to allow for cellular differentiation of bronchial epithelial cells. Such cultures represent a reasonable model of the pseudo-stratified, columnar epithelium found in the upper airways.[55] When grown at an air-liquid interface for a minimum of 21-28 days, NHBE cells develop a polarized, pseudo-stratified structure accompanied by the appearance of basal-like, mucus-secreting, and ciliated cell types.[55] By culturing the cells upon a semi-permeable membrane, PM can be deposited directly upon the apical surface of the cell layer as seen below in Figure 2.[56]

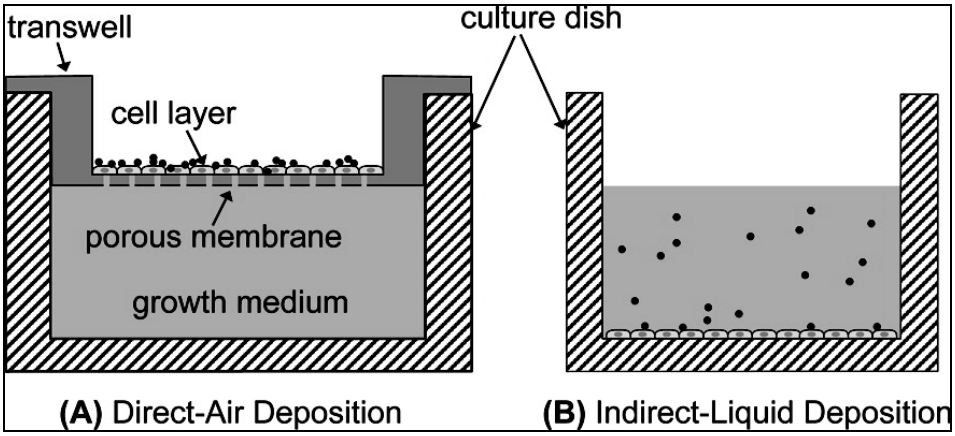

Figure 2. Comparison of in vitro exposure techniques (A) The novel technique of direct deposition of PM (black circles) onto the apical surface of the cell layer (B) Conventional technique of indirect-liquid deposition.[56]

1.7.4. Electrostatic Aerosol In vitro Exposure System (EAVES)

Several new systems have recently been developed to expose cultured human airway

cells to aerosols.[56, 57, 58] Storey et al. developed a direct air to cell deposition system whereby cells grown at an air liquid interface were exposed to diesel exhaust in an exposure chamber heated and humidified to physiological temperature and relative humidity. However the system relied solely upon settling and Brownian motion to deliver particles to cell surfaces, which severely limited the rate of particle deposition. This system, therefore, required long exposure durations at high PM concentration.[58] An alternative technique utilizes electrostatic precipitation to deposit aerosols upon cells. Electrostatic precipitation of aerosols onto cells grown at air-liquid interface has several advantages: (1) the physical and chemical characteristics of the aerosol like size, surface area, and chemical constituency are better maintained than when aerosols are collected on a filter substrate and resuspended in an aqueous medium and (2) electrostatic precipitation offers a greater deposition efficiency than techniques which rely upon gravitational settling or diffusion. A modified version of the electrostatic aerosol in vitro exposure system first developed by de Bruijne et al.[59] is shown in Figure 5.[56]

One possible disadvantage of using electrostatic charging for aerosol deposition is the creation of ozone during electrostatic charging. As oxygen in the air passes through the corona charger, ozone is created. Ozone generation is a concern because ozone is a potent oxidant, capable of inducing stress in airway cells and exacerbating the inflammatory effects of ambient PM inhaled by humans.[60] However, previous experiments run with similar flow rates and charging conditions reported no significant detrimental effects upon NHBE cells.[56]

1.8. Traditional versus Improved Cook stoves

Improved stoves are typically evaluated for their emissions and fuel reductions relative to the emissions and fuel consumption of a traditional "three-stone fire". The three stone fire represents a traditional open fire burned in homes where stoves are not available or not affordable. In this research, the three-stone fire was used as a traditional stove model, in conjunction with two improved stove models: the Envirofit G3300 single pot stove and the Philips Gasifier wood stove.

Envirofit's G3300, single pot stove, can be seen in Figure 3 below. [61, 62] The G3300 stove has a rocket-elbow combustion chamber design. The L-shape of the rocket elbow allows for a chimney effect within the combustion chamber. As the wood is burned, a strong upward draft is created from the rise of the heated air. The upward draft within the chimney pulls air through the fuel chamber which allows for improved fuel and air mixing, thereby allowing the wood to burn more efficiently. The rocket elbow design includes a small opening where wood fuel can be fed into the combustion chamber in a more controlled fashion. Together, these design modifications increase fuel efficiency and reduce carbon monoxide and particulate matter emissions.

Figure 3. Envirofit's G3300 single pot stove[61, 62]

The Philips Gasifier stove, shown in Figure 4, was selected as the second improved cook stove for this study. The gasifier design is based upon a two-stage combustion system. At the base of the combustion chamber, wood fuel is burned with limited air to allow for pyrolysis. The smoldering fuel bed produces tars, high carbon content charcoal, and low molecular weight gases. As the gases rise through the chamber, they are mixed with oxygen from a secondary air intake. The oxygen reacts with the low molecular weight gases to produce CO, CO_2, H_2, and CH_4. By separating the combustion into two stages, the gasifier allows for an improved air and fuel mixing (mixing air with fuel gases in the second stage) and a more complete combustion reaction, thereby reducing fuel consumption and carbon monoxide and particulate matter emissions.

Figure 4. The Philips Gasifier wood stove[61, 62]

1.9. Objective of this Research

Although the emissions and the cost of fuel for each stove can be easily quantified, the potential for each stove to improve human health is not as easy to quantify. Therefore, the full benefit from global dissemination of more efficient stoves remains to be seen, especially in terms of a public health impact. From a health standpoint, the improved cook stove hypothesis states that the use of an improved stove should result in a commensurate improvement in the health of the user and their family. This study sought to test one aspect of that hypothesis by evaluating the inflammatory response of human lung cells exposed to biomass combustion emissions in a controlled laboratory setting.

2. Materials and Methods

2.1. Epithelial Cell Culture

Normal human bronchial epithelial (NHBE) cells were obtained by brush biopsy from two healthy, non-smoking adult human volunteers (EPA, Chapel Hill, NC) and from purchase through the Lonza corporation (Lonza, Walkersville, MD).[63] The cells were cryopreserved and shipped to Colorado State University where they were stored at -80ºC for 24 hours before being placed in liquid nitrogen for storage. Four to six weeks prior to exposure, the cells were thawed, centrifuged, and resuspended in Bronchial Epithelial Growth Medium (BEGM kit, Lonza, Walkersville, MD).[64] Cell solutions were supplemented with 5 mL of antibiotic/antimycotic solution (100 U penicillin/milliliters, 100 micrograms streptomycin/milliliter) (Gibco, Invitrogen, Carlsbad, CA) before being plated onto sterile Petri dishes at a seeding density of approximately 25,000 – 35,000 cells per cm^2. The cells were incubated at 37 ºC in a five percent CO_2:air atmosphere until confluent, as confirmed using transmitted light microscopy. Once confluent, the cells were harvested (Cell Detachment Solution, Hyclone, Waltham, MA), counted, and re-plated onto additional culture dishes. Growth medium was replaced every 48 hours. This process was repeated until a total cell count of approximately $5 \cdot 10^6$ was achieved. The NHBE cells were then detached from the Petri dishes using HyQtase, centrifuged, and resuspended into 9 mL of air-liquid interface medium (ALI media) that consisted of 50% DMEM-H, 50% BEBM, one complete BEGM bullet kit (per 500 milliliters media), and one additional bovine pituitary extract singlequot (13 mg/mL) (all from Lonza,

Walkersville, MD). One hundred and fifty microliters of cell solution was then plated onto porous, polycarbonate membranes (0.4 micrometer pore diameter Snapwell, Corning Inc) to achieve a cell seeding density of approximately 70,000 cells per cm^2. A total of 60 air-liquid interface wells were prepared in this manner. The porous polycarbonate membranes had been previously coated with a 0.04 mg/mL solution of Rat Tail Collagen Type I suspended in BEGM media 12-24 hours prior to cell seeding. The bottom compartment of each snapwell was filled with 4 mL of ALI media.

Once the NHBE cells achieved confluence, both the apical and basolateral media were removed and replaced with air-liquid interface (ALI) media supplemented with 500 nM retinoic acid (RA). The basolateral compartment was refilled with four milliliters ALI + 500 nM RA media, and the apical compartment was refilled with 200 µL ALI + 500 nM RA media. Approximately 48 hr later, the culture was taken to air-liquid interface by replacing the basolateral compartment with 4 mL of ALI media supplemented with 100 nM RA. The apical compartment remained unfilled and exposed to air. This process established day zero of the air-liquid interface culture. Cells at ALI were rinsed with phosphate buffered saline solution (Hyclone, Waltham, MA) at days 10 and 18 of ALI. The air-liquid interfaced cells were exposed to cook stove emissions between days 23 and 28 of ALI.

2.2. Paraffin Embedding of Cells at Days 1, 10, 24, and 28 of ALI

On days 1, 10, 24, and 28 of air-liquid interface, one snapwell membrane was fixed with formalin and paraffin embedded to observe signs of progressive cell differentiation. Paraffin-embedded cultures were sectioned on a microtome, affixed to a microscope slide, and stained with hematoxylin and eosin using a standard procedure (Todd Bass,

Veterinary Diagnostic Lab, CVMBS, Colorado State University). Slides were then imaged using transmitted light microscopy at 312x magnification (Leitz Light Microscope, Orthoplan, Germany; SPOT RT Slider Camera, SPOT imaging solutions, Sterling Heights, MI).

2.3. Electrostatic Aerosol in Vitro Exposure System (EAVES)

Air-liquid interface cultures were exposed to cook stove emissions using an electrostatic aerosol in vitro exposure system (EAVES). A schematic of the EAVES is shown in Figure 5 below. This system was first described by De Bruijne et al.[59] and was subsequently modified by Volckens et al.[56]

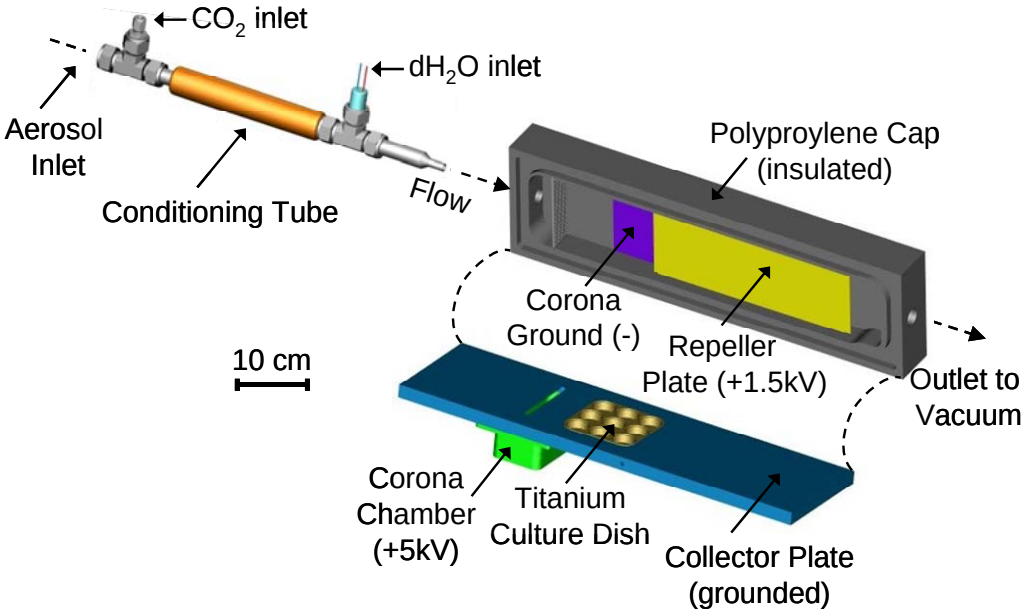

Figure 5. The electrostatic aerosol in vitro exposure system (EAVES) [56]

Aerosol entering the EAVES was heated to 37.4 ºC and humidified to 85% relative humidity to enhance cell viability during exposures. A corona source, located immediately downstream of the conditioning tube applied a positive charge to the

aerosol, which was then precipitated onto the cell culture using a repeller plate charged to + 1.5 kV. Up to nine air-liquid interfaced cultures could be exposed at a single time within the EAVES. Airflow was regulated at 4 L/min by a mass flow controller (FMA 5400/5500, Omega Engineering, Inc.) that was previously calibrated with a primary flow standard (DryCal DC-2, Bios International Corporation). A syringe filled with distilled water was used to humidify the incoming aerosol by delivering water to the conditioning tube at a rate of 0.146 – 0.156 mL/min. The syringe flow rate was controlled by a Harvard Syringe Pump (PHD 22/2000 Syringe Pump Series, Harvard Apparatus, Holliston, MA) and was determined based upon the ambient relative humidity and temperature, the desired relative humidity and temperature within the aerosol chamber (typically 80-90% for optimal cell viability) and the airflow rate through the EAVES. Temperatures within the exposure chamber were maintained using a thermistor-PID controller (Omega Multizone Ramp and Soak Controller, CN1500 Series, Omega Engineering Inc.) in conjunction with several resistive heaters. The temperature of the aerosol conditioning tube at was maintained at 38°C (zone 1), the corona charger region was maintained at 34°C (zone 2), and the area near the exit of the chamber was maintained at 31°C (zone 3). Air exiting the chamber was passed through a series of cooling coils and the condensate was collected in a dessicator loaded with pre-baked silica quartz. A final water catch was installed in line prior to the air flow pump to further minimize moisture interference with pump function.

2.3.1. Collection Efficiency of the EAVES

Aerosol collection efficiency in the EAVES was evaluated prior to lung cell exposures. For these tests, the EAVES was operated with a corona current of 10 μA, an

electrical field strength of 1.5 kV, and an aerosol flow rate of 4 L/min. Relative humidity within the EAVES was maintained between 80 and 90%. Zone temperatures (zone 1: 38°C, zone 2: 34°C, zone 3: 31°C) were set to maximize particle collection efficiency while remaining close to the physiological optimal temperature of 37.4°C. Each collection efficiency test lasted approximately four to six hours.

Biomass combustion aerosols were generated by burning a single incense stick inside a 1.3 m^3 chamber. Particle collection efficiency in the EAVES was determined with and without power applied to the corona and repeller regions. The former condition (power on) was used to characterize collection efficiency under normal operating conditions, while the latter condition (power off) provided an indication of particle losses within the EAVES. Particle losses were determined by differential count of aerosol concentration upstream and downstream of the device using a condensation particle counter (CPC, Grimm Technologies Inc., Douglasville, GA) and with the charger and repeller off. Particle losses were calculated using Equation 1,

$$\ell = \frac{C_{up} - C_{down}}{C_{up}} \qquad (1)$$

where ℓ represents losses, C_{up} represents the particle count upstream of the EAVES and C_{down} represents the particle count downstream of EAVES.

Particle collection efficiency was measured with the corona charger and repeller turned on with the CPC downstream of the EAVES chamber. Total particle collection efficiency, E, by particle number concentration was determined by Equation 2,

$$E = \left[1 - \left(\frac{C_{on}}{C_{off}}\right)\right] \times 100 \qquad (2)$$

where C_{on} represents the concentration of particles exiting the EAVES chamber with the repeller on, and C_{off} represents the concentration of the particles exiting the EAVES chamber with the repeller off.

A second round of efficiency tests was then conducted to determine the relative flux of aerosol to a given collection area within the EAVES. The objective of these tests was to determine the uniformity of particle collection across the cell culture growth area. These tests were conducted under the same operating conditions as the collection efficiency tests, except that ammonium fluorescein was used as the test aerosol. Aluminium foil was placed above the particle collection region (extending from the corona charger to the exit of the exposure chamber). Ammonium fluorescein aerosol was generated by nebulizing a suspension of fluorescein powder within an aqueous ammonia solution to achieve a 2:1 ratio of fluorescein to ammonium hydroxide and a pH of approximately 12. Each collection uniformity test lasted approximately 30 minutes. The foil was then carefully removed and cut into pieces representing each culture well position within the nine-well titanium dish. The fluorescein was extracted using an ammonium hydroxide solution and the relative fluorescence was measured using a fluorescent plate reader (FLX-800, BioTek Inc, Winooski, VT). Aluminium foil substrate

blanks were taken on a daily basis. This procedure was repeated four times; surfaces within the EAVES were cleaned with a 70% ethanol solution between repetitions.

The percent deposition of aerosol into each well of the cell culture exposure plate, D_i, was determined by Equation 3,

$$D_i = \frac{F_i}{\sum F} \times 100 \qquad (3)$$

where F_i represents the fluorescence measured in each well location, and $\sum F$ represents the sum of all fluorescence measured within the EAVES chamber.

2.4.Wood Smoke Generation and Exposures

All cook stove emissions testing and exposures were conducted at the CSU Engines and Energy Conversion Laboratory. The cook stoves were tested within a constant displacement fume hood (Figure 6) operated at a flow of 6000 L/min. The hood dimensions were: 1.2 m x 1.2 m x 4.3 m. The top of the hood was fitted with a cap to exhaust the air through a 12.7 cm diameter duct. The base of the hood was equipped with a HEPA filter to remove background aerosol from the incoming air.

Figure 6. The fume hood used for cook stove emissions testing at the EECL[65]

Gaseous emissions were measured using a Fourier Transform Infrared Spectrometer (FT-IR). Standard methods were followed in the construction of a stainless steel sample probe used for analyzing the gases.[66] On each day of testing, the FT-IR was zeroed and calibrated according to a standard protocol before the cook stove tests were begun.[66]

A 38.1 cm long stainless steel probe with an inner diameter of 0.5 cm connected exhaust from the top of the fume hood to a 1.0 cm outer diameter sample line, which directed 4 L/min of flow into the EAVES. The velocity within the fume hood exhaust pipe was 25.26 m/sec. Due to probe size and air flow restrictions, isokinetic sampling was not feasible. The Stokes number for the median particle size sampled was less than 0.0005, which would cause minimal error due to anisokinetic sampling. Although the majority of the particles produced from combustion were in the submicrometer size range, it is possible that there were particles in the coarse size range (> 1 μm) emitted

from the stoves. The concentration overestimate error due to the EAVES subisokinetic sampling conditions would have been as high as factor of 5 for a 10 μm particle.

For the cell exposures, the EAVES chamber was operated between 80 and 90% relative humidity, and the temperatures at zone 1, zone 2, and zone 3 were maintained at 38ºC, 34ºC, and 31ºC respectively. Medical grade CO_2 (Airgas, Inc.) was delivered to the EAVES at a flow rate of 0.2 L/min to allow the cells to maintain physiological pH. The total flow rate through the EAVES was checked and adjusted using a DryCal flow meter (DryCal DC-2, Bios International Corporation) before and after each stove exposure. The experimental matrix for the cell exposures is shown in Table 1 below.

Experimental Variable	Number of Variables	Level of Variation
Normal Human Bronchial Epithelial Cells	3	Donors 1, 2, 3
Stove Type	4	Improved Stoves (2), Three-stone fire (1), Room Air Controls (1)
Experimental Repetitions	n/a	NHBE cells (3) exposed to each stove type (4) twice
Cellular Marker Timepoints	2	1, 24 hrs Following Exposure
Cellular Markers	5	GAPDH IL-8 HOX-1 COX-2 LDH

Table 1. The experimental matrix for normal human bronchial epithelial cells exposure to cook stove emissions, and post exposure biomarker analysis

On each test day, a stove model was randomly selected, and a standardized water boil test was begun by following a protocol similar to the water boil test used by Household

Energy and Health Programme, Shell Foundation.[67] The stove was placed in the fume hood and a 6 L water pot with 5 kg of water was placed upon the stove. Wood fuel was weighed before each burn. Douglas fir with a 7% moisture content was used as fuel for both the Envirofit G3300 stove and the three stone fire. West Slope Pellets with moisture content of 6.4%, a carbon content of 49.2% by mass, and a nitrogen content of 0.1% by mass were used as fuel for the Philips Gasifier stove. The fire was maintained and fed with wood fuel until the water in the pot was brought to a boil. Once boiling, the pot was maintained at a simmer for forty-five minutes. The total wood fuel consumed during the simmer phase (45 minutes) was recorded. Wood smoke from the simmer phase was used for the cell exposures.

Measurements of the ambient relative humidity and temperature were taken while waiting for the water pot to reach boil. These measurements were used to calculate the syringe flow rate necessary to achieve approximately 80-90% relative humidity within the EAVES chamber. Once the simmer phase began, EAVES mass flow controller and air flow pump were turned on. Next, the CO_2 mass flow controller was turned on and the CO_2 delivery valve was opened. The flow upstream of the EAVES chamber was measured using a DryCal flow meter (DryCal DC-2, Bios International Corporation). The mass flow controller was then adjusted to obtain a total flow of 4 L/min through the EAVES chamber. The thermocouple device responsible for heating and controlling the temperature at zones 1, 2, and 3 was turned on and allowed to heat zone 1 to 38ºC, zone 2 to 34ºC, and zone 3 to 31ºC. The water syringe pump was turned on and the syringe pump rate was set to achieve approximately 80-90% relative humidity within the EAVES. Once the pot had arrived at a simmer, six NHBE cell culture wells at day 21-28

air-liquid interface were placed within the nine-well titanium dish in the pre-warmed, pre-humidified EAVES. The arrangement of the cell culture wells within the nine-well titanium dish is shown below in Figure 7.

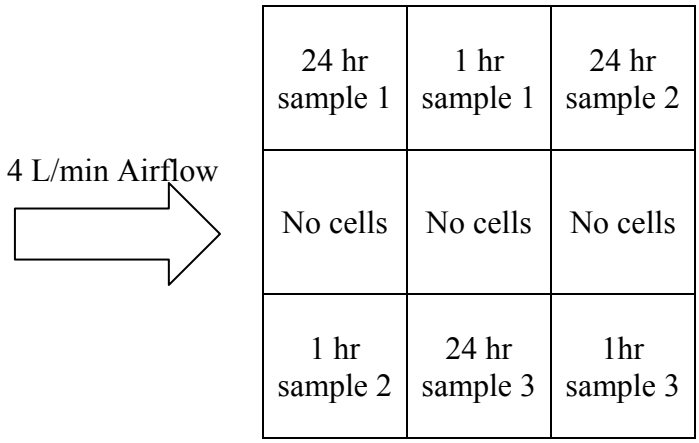

Figure 7. The arrangement of the cell samples within the EAVES exposure chamber titanium plate

Once the culture wells were placed within the chamber, the charger and repeller were turned on. The charger was maintained at 10 μA while the repeller was maintained at 1.5 kV. The repeller electric field was periodically measured using a Voltmeter (Omegaette HHM93, Omega Engineering, Inc.) The cells were exposed to the cook stove emissions for 45 minutes. At the conclusion of the exposure, the charger and repeller were turned off and the cell cultures were transported to and stored in an incubator until further analysis (see Section 2.7). This procedure was repeated for the remaining two stove models. The fume hood was cleared between each stove test by waiting approximately 15-20 mins. The same procedure was repeated for the control cells with two exceptions: (1) no stove was burned in the fume hood; filtered, room air was pulled through the EAVES and (2) the charger and repeller were kept off such that no electrostatic

precipitation of the ambient aerosols occurred. All other settings for the EAVES were kept the same for the controls.

This procedure took about 12 hours to expose cells from the donor 1 phenotype to the three stove models and the control (room air). The procedure was repeated two days later with fresh (unexposed) ALI cells from the same donor 1 phenotype. The testing procedure was repeated for each phenotype, with each of the three phenotypes being exposed to the three stove models and room air twice. A total of six days of stoves testing was required to complete 24 cell exposure experiments (3 donors x 4 stove types x 2 repetitions).

2.5. Analysis of Cook Stove Emissions

2.5.1. Particle Size Distribution

The particle size distribution emitted by each stove was measured with a Sequential Mobility Particle Sizer (SMPS+C, Grimm Technologies, Douglasville, GA). The SMPS calculates particle diameter based upon the mobility of a particle in an electrical field, assuming a spherical particle shape and standard density (1 g/cm^3). Particles entering the SMPS were neutralized to achieve a Boltzmann charge distribution, before being flowed through the electrostatic classifier section. A central rod within the electrostatic classifier section was charged with a voltage that cycled from 20 to 10,000 Volts. At the bottom of the rod was a small exit slot where particles of selected electrical mobility were allowed to pass. Modulation of the rod voltage allowed particles of varying mobility diameter to pass through the exit slot, allowing particles between 5 and 1110 nanometers to be size-selected over a period of several minutes. A condensation particle counter measured the concentration of particles within each size range as they exited the electrostatic classifier

section, allowing the SMPS to determine the aerosol size distribution emitted from each cook stove.

To achieve a representative aerosol sample for SMPS measurements, a 19 L sample reservoir was constructed. Air was pulled from the exhaust pipe into the sample reservoir by a pump rated to pull air at 0.76 m^3/min. Air was pulled into the sample reservoir for approximately seven minutes before the pump was turned off and the SMPS turned on. The SMPS then sampled aerosol collected in the sample reservoir. After completing a scan, the SMPS was disconnected from the bucket and a room-air scan was conducted while the 19 L reservoir was refilled. This procedure was repeated two to three times for each cook stove exposure.

2.5.2. Gravimetric Analysis of Cook Stove Emissions

Particulate matter emissions smaller than 10 μm (PM_{10}) were collected on 47 mm Teflon filters (PALL, LifeSciences, Ann Arbor, Michigan) following a protocol similar to that of Subramanian et al.[68] The sampling train consisted of a 0.5 cm diameter stainless steel probe that directed flow into two filter collection cassettes in parallel. One collection cassette collected PM_{10} upon a 47 mm Teflon filter with a pre-baked 47 mm quartz filter (PALL LifeSciences, Ann Arbor, Michigan) in line behind the Teflon filter. The second collection cassette collected PM_{10} upon a pre-baked quartz filter alone. Only the Teflon filter gravimetric analyses were used for this investigation.

The total flow through both filter cassettes was 17.35 L/min which was within 10% of the flow rate needed for isokinetic sampling. The total flow rate through the cassette containing the Teflon filter for gravimetric analysis was 8.4 L/min. A PM_{10} cyclone (URG-2000-30ENB, URG Corp, Chapel Hill, NC) was placed in the sampling line to

limit filter collection of particles to particles that were smaller than 10 micrometers in diameter. Gravimetric analysis of the filters was used to estimate the total PM_{10} emitted from each cook stove model during the duration of each exposure test.

The time-weighted average concentration of PM_{10} in the cook stove emissions, $[PM_{10}]$, was calculated using Equation 4,

$$[PM_{10}] = \frac{PM_{10}}{V_{total}} \qquad (4)$$

where $[PM_{10}]$ represents the estimated concentration of PM_{10} in the cook stove emissions in micrograms/m^3, PM_{10} represents the mass of PM_{10} collected upon the Teflon filter in micrograms, and V_{total} represents the total volume of air, in cubic meters, that passed over the Teflon filter during a test.

2.6. Estimation of PM_{10} Mass Delivered to Cells

The mass of particles deposited per unit growth area of the NHBE cells (PM_{dep}) was calculated from Equation 5,

$$PM_{dep} = \frac{[PM_{10}] \cdot Q_E \cdot t \cdot E \cdot D_i}{A_{growth}} \qquad (5)$$

where $[PM_{10}]$ represents the estimated PM_{10} concentration in the emissions from each cook stove (Equation 4), Q_E represents the flow through the EAVES chamber in cubic meters per minute, t represents the duration of exposure in minutes, E represents the fractional collection efficiency of the EAVES, D_i represents the estimated particle

deposition on the i^{th} cell culture well as a fraction, and A_{growth} represents the area of cellular growth in centimeters squared.

2.7. Cellular Markers

2.7.1. Cell Viability

Lactate dehydrogenase (LDH) assays are used as a measure of cell death. Lactate dehydrogenase is expressed universally in all cells. The loss of membrane integrity during cell death causes extracellular release of LDH. The amount of LDH released is proportional to number of dead cells, allowing for LDH to be used as an indicator of cytotoxicity.[69] The cell viability of the exposed and control cells was assayed at 1 and 24 hours post exposure by using an LDH assay and standardized protocol (Promega Cytotox96 Non-radioactive Cytotoxicity Assay). The percent LDH released was calculated using Equation 6,

$$\%LDH = \frac{LDH_{\exp osed}}{LDH_{\max}} \times 100 \qquad (6)$$

where *%LDH* represents the percent LDH released, $LDH_{exposed}$ represents the estimated LDH released in the cell exudate, and LDH_{max} represents the maximum amount of LDH released from cells (estimated during the assay).

2.7.2. Cellular Inflammatory Response

Total mRNA transcripts from exposed and control cells were isolated at 1 and 24 hours following exposure using a standardized kit and protocol (RNeasy mini kit, Qiagen,

Valencia, CA). A DNase digestion step was added to minimize the risk of DNA contamination (RNase Free DNase Set, Qiagen, Valencia, CA). The purity and quantity of mRNA was assessed by spectrophotometry at wavelengths of 260 and 280 nm (Nanodrop ND-1000, ThermoScientific, Wilmington, DE). Transcripts were stored at -80ºC for 4-6 weeks prior to analysis with real-time RT PCR. A standard real-time RT PCR protocol (Biorad One-Step RT-PCR Kit with SYBR Green, Bio-Rad Laboratories, Hercules, CA) was followed to amplify the three genes of interest: Interleukin-8 (IL-8), cyclooxygenase-2 (COX-2), and heme oxygenase-1 (HOX-1). Gene expression levels were normalized to the expression of glyceraldehyde 3-phosphate dehydrogenase (GAPDH), which is expressed universally in NHBE cells.

Primers were designed for IL-8, COX-2, HOX-1, and GAPDH. The reliability of the primers was tested through the generation of standard curves prior to analysis. The nucleotide sequences for each primer are provided in Appendix A. All samples were processed through a real-time RT PCR machine (iCycler, BioRad, Hercules, CA). A water blank and a non-reverse transcriptase blank were processed with each sequence to check for DNA contamination of reagents and samples, respectively.

2.8. Statistical Analyses

All statistical analyses were conducted with SAS software (SAS Institute Inc., Cary, NC). Statistical significance was evaluated with a type I error rate of $\alpha=0.05$ for all analyses. Total particle counts, particle count median diameters, PM_{10} mass, and PM_{10} mass concentration emitted by each stove during the simmer test were compared using a one-way ANOVA MEANS procedure in SAS. The mean fuel consumption and emissions factors for each stove were compared using the same procedure.

Since the cellular release of LDH and the cellular expression of IL-8, HOX-1, and COX-2 at one and twenty-four hours post exposure data relied upon time series data, a mixed linear model was chosen. The MIXED procedure in SAS was used to evaluate the fixed effects of stove model, time point post-exposure, and their interactions. The random effects of NHBE donor and burn day were also evaluated using the same procedure.

All emissions and cellular inflammatory response data were log transformed to satisfy the model assumptions of normality and homoscedasticity. A plot of the residuals was used to evaluate the homoscedasticity assumption. A Tukey's adjustment was made to account for the error due to multiple comparisons.

3. Results and Discussion

3.1. Air-Liquid Interfaced NHBE Cells

The physical progression of the NHBE cells grown at an air-liquid interface is shown in Figure 8. The NHBE cells underwent progressive differentiation over the course of 24 days. By day 24, cell cultures demonstrated a pseudo-stratified columnar epithelium with signs of basal, goblet, and ciliated cell types. Basal cells exist as the bottom layer of lung epithelial cells. In the body, basal cells serve to attach lung epithelium to the basal lamina and underlying mesenchymal structures.[70] In the in vitro model used for this study, the basal cells served to attach the lung epithelium to the collagen coated membrane. The goblet cells are secretory cells that secrete mucus (blue lining of apical surface of cells in Figure 8). In the body, ciliated cells propel mucus upward to the pharynx and out of the airways.

Day 1 of ALI:
Squamous layer
of NHBE cells

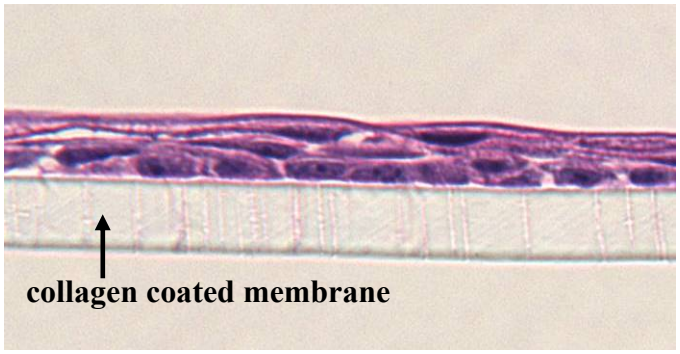

Day 10 of ALI:
Progressive
differentiation

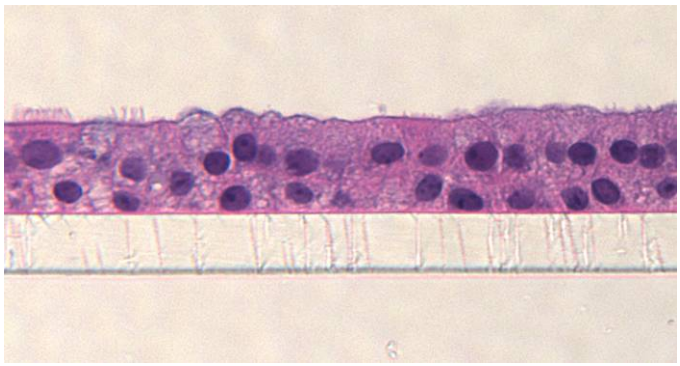

Day 24 ALI:
Pseudo-stratified
columnar
epithelium.
Signs of basal,
goblet, and
ciliated cell
types.

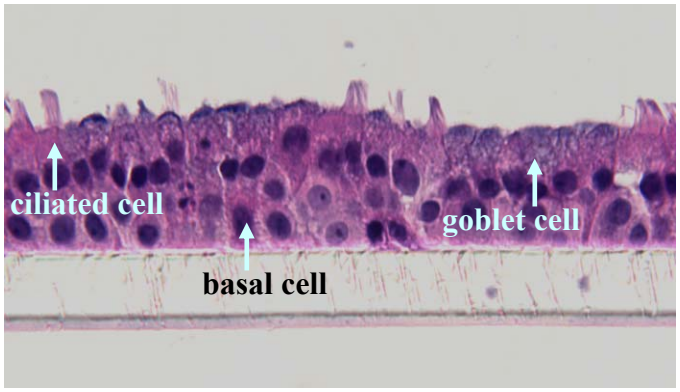

Figure 8. Formalin fixed and paraffin-embedded sections from air-liquid interfaced cultured NHBE cells grown upon a collagen coated membrane. Cells were treated with a hematoxylin and eosin staining procedure. Images are shown at 312x magnification.

3.2. Collection Efficiency and Percent Deposition within the EAVES

Particle collection efficiency of the EAVES ranged from 65-80% when operating with settings identical to those used for the cook stove exposures. Particle losses within the EAVES were negligible.

The average percent deposition of ammonium fluorescein particles into the cell culture wells ranged from 4.2-5.6%, as shown in Figure 9. Of the nine culture well regions in the EAVES, the upper three wells and lower three wells were the most similar and consistent in their collection of deposited fluorescein. The upper and lower wells thus served as the housing sites for the six culture wells during actual cook stove tests.

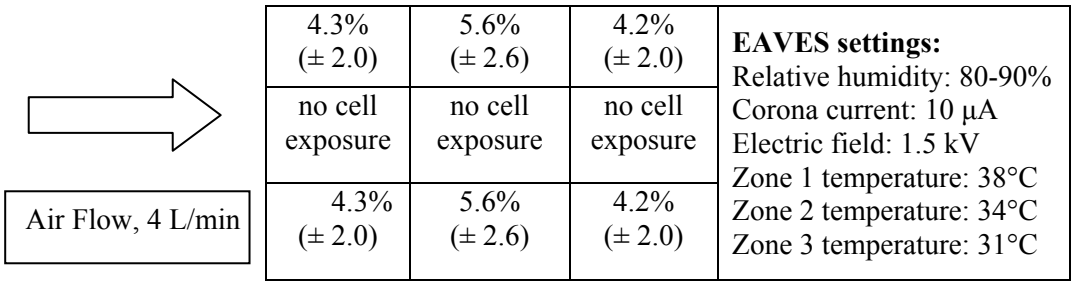

Figure 9. Average percent deposition (± one standard deviation) of ammonium fluorescein aerosol to each cell culture well in the nine well cell culture plate within the EAVES.

3.3 Cook Stove Emissions and Estimated PM_{10} Mass Delivered to Cells

The particle size distributions emitted by each stove type are shown in Figure 10 below. The particle size distribution is based upon the electrical mobility size as measured by the Sequential Mobility Particle Sizer (SMPS) during the cook stove tests.

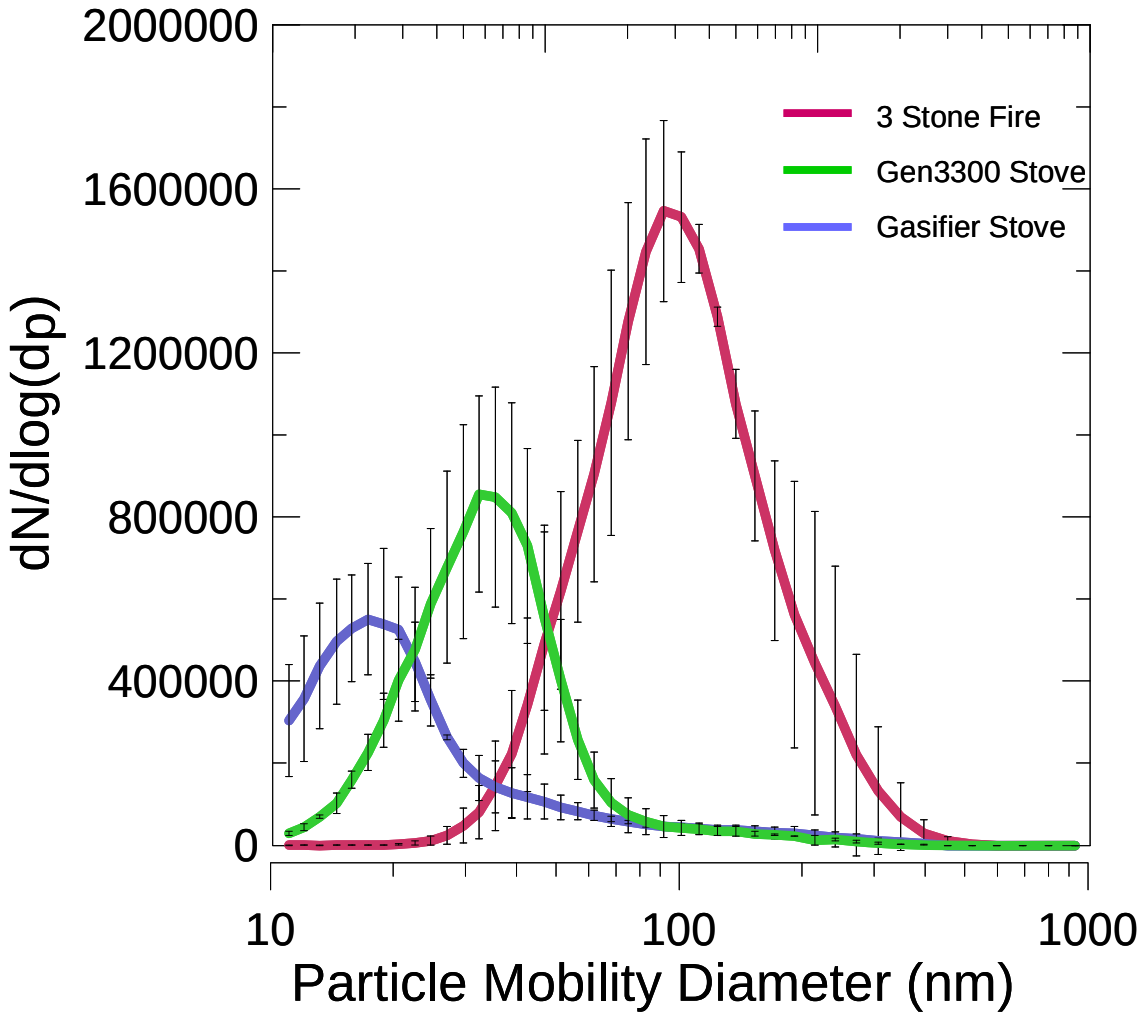

Figure 10. Particle size distributions emitted during the simmer phase for each of the three stoves. Error bars represent one standard deviation.

The Philips Gasifier produced the fewest and smallest diameter particles. The Philips Gasifier produced approximately $6.5 \cdot 10^6$ particles/cm^3 ($\pm$ $8.0 \cdot 10^5$) with a count median diameter (CMD) of 19.4 nm ($\pm$ 1.8 nm). The Envirofit G3300 stove produced more particles and particles of a larger mobility diameter than the Philips Gasifier. The Envirofit G3300 stove produced $7.8 \cdot 10^6$ particles/cm^3 ($\pm$ $1.4 \cdot 10^6$) with a CMD of 26.0 nm

(± 3.3 nm). Yet, there was no statistical difference between the Philips Gasifier and the Envirofit G3300 stove with regard to CMD or particle count per cubic centimeter (α = 0.05). The three stone fire produced the largest number of particles and particles with the largest CMD. The three stone fire produced approximately $1.78 \cdot 10^7$ particles/cm^3 (± $8.9 \cdot 10^5$) with a CMD of 92.3 nm (± 13.0) nm, both of which were significantly elevated above the CMD and particle count observed for the Philips Gasifier and Envirofit G3300 stove.

The means for the total PM_{10} mass collected upon Teflon filters, the estimated total PM_{10} mass emitted, the concentration of PM_{10} in the exhaust flow, the wood fuel consumed, and the emissions factor for each stove during the simmer phase of the water boil test can be seen in Table 2 below.

Stove	**Sampled PM_{10} (µg)**	**Total PM_{10} (µg)**	**[PM_{10}] (µg/m^3)**	**Fuel Consumed (g)**	**Emissions Factor (PM_{10}/Fuel) (µg/g)**
Three Stone Fire	1660 (± 405)	26400 (± 6430)	4410 (± 1070)	523 (± 14)	51 (± 13)
Envirofit G3300	457 (± 28)	7260 (± 437)	1210 (± 73)	314 (± 12)	23 (± 2)
Philips Gasifier	187 (± 52)	2970 (± 830)	495 (± 138)	195 (± 15)	15 (± 3)

Table 2. The total PM_{10} mass sampled, the total PM_{10} emitted, the average concentration of PM_{10} in the exhaust flow, the mass of fuel consumed, and the emissions factor for each stove during the simmer phase of the water boil test. One standard deviation is shown in parentheses.

As can be seen in Table 2 above, the three stone fire produced approximately three times more PM_{10} mass than the Envirofit G3300 stove and approximately eight times more PM_{10} mass than the Philips Gasifier produced during the simmer phase. The Envirofit G3300 stove produced approximately 2.5 times more PM_{10} mass than the

Philips Gasifier. The PM_{10} mass emitted from each of the stove models differed significantly at the 95% confidence level.

The total PM_{10} released by each stove did not account for the varying amount of wood fuel needed to maintain a six liter pot of water at a simmer for 45 minutes. Fuel consumption during the simmer test for each stove differed significantly at the 95% confidence level, which was not surprising given varying heat transfer capabilities and combustion efficiency differences between the three stoves tested. The three stone fire consumed 1.7 times as much wood fuel as the Envirofit G3300 stove, and 2.7 times as much wood fuel as the Philips Gasifier. The increased fuel consumption may be explained by the reduced heat transfer to the water pot. The three stone fire is built to resemble an open fire in a home, much like a typical campfire, with little to no elevation between the wood fuel and the ground. Such construction leads to a loss of thermal energy to the ground through convection.

Typical PM levels in households with open burning range have been found to range from 100 to 1000-2000 $\mu g/m^3$, with peaks during cooking reaching levels five to ten times higher (Smith 2008). A study in rural Kenya found that traditional open fires users' average daily PM_{10} exposure to be 4,898 $\mu g/m^3$.[71] The WHO found that 24 hour levels of PM_{10} in homes using biomass fuels reach 300-3000 $\mu g/m^3$ with spikes reaching as high as 10,000 $\mu g/m^3$ during cooking.[72] The PM_{10} mass concentration observed during cellular exposure to emissions from the 3SF corroborates with PM_{10} concentrations observed during peak cooking use in homes with open fires.

The higher PM_{10} mass concentration (Table 2), particle counts and particle mobility diameters (Figure 10) emitted from the three stone fire could have been due to (1) a larger quantity of wood fuel needed to maintain a pot of water boiling for 45 minutes (decreased heat transfer) and/or (2) a decreased combustion efficiency, relative to the other stove models tested. The stove emissions factor (PM mass emitted per mass of fuel consumed) is a useful measure of the combustion efficiency of a stove as it normalizes PM mass emissions to fuel consumed thereby minimizing the effects of heat transfer and fuel consumption differences upon PM mass emissions. When considering the emissions factors seen in Table 2, it can be inferred that not only did the three stone fire consume the most wood fuel per task, but it emitted significantly more PM_{10} mass per gram of wood fuel than either of the other two stove models tested (95% confidence level). The three stone fire produced two times as much PM_{10} mass per gram of wood fuel as the G3300 stove, and three times as much PM_{10} mass per gram of wood fuel as the Philips Gasifier during the simmer phase. The increased fuel consumption and the higher emissions factor for the three stone fire may be due to its reduced heat transfer and combustion inefficiency. A three stone fire is constructed by placing the wood fuel directly upon the ground. This construction allows for little control over the air and fuel mixing and the lack of control over the air and fuel mixing can lead to a reduced combustion efficiency.[73] The emissions factor data and knowledge of the improper air to fuel mixing in the three stone fire suggest that there is a larger proportion of wood fuel consumed in the three stone fire that remains incompletely oxidized, relative to the other two stoves.

The increase in fuel consumption and the reduced combustion efficiency of the three stone fire may explain the increased PM_{10} mass emissions and the larger mobility size of particles emitted from the three stone fire. The PM_{10} mass emitted per gram of wood fuel consumed did not differ significantly between either of the two improved stoves (95% confidence level). However, the G3300 stove did consume significantly more wood fuel than the Philips Gasifier, which helps to explain the increase in the total PM_{10} mass emitted from the G3300 stove, and the increased estimated PM_{10} mass delivered to the NHBE cells during cook stove exposure tests (see Table 3 below), relative to the Philips Gasifier.

The fewer number and smaller mobility sizes observed for the particles produced from biomass burning in the Philips Gasifier may be explained by the improved fuel and air mixing technique utilized in gasification. Gasification allows for improved fuel and air mixing by separating the biomass burning into two combustion stages. In the first stage the solid wood fuel is pyrolized into tar, high density charcoal, and low molecular weight gases. The low molecular weight gases rise and are then mixed with incoming air, allowing for a more thorough oxidation of the combustion products. A more thorough oxidation of the combustion products leads to reduced PM emissions. However, the use of West-Slope pellets as the wood fuel for the gasifier stove may have also affected the observed variation in particulate size, count, and mass, when compared to the emissions from the G3300 stove, which burned Douglas fir.

The rocket elbow design of the combustion chamber in the G3300 stove also allowed for a more controlled wood fuel feeding and fuel to air mixing; however the pyrolysis and gasification steps of combustion were not as spatially separated as in the Philips Gasifier

and the oxidation of the wood fuel in the G3300 stove may not have been as complete. This likely resulted in particles that were larger in diameter and more numerous when compared to the Philips Gasifier PM emissions. However, due to the limitations in experimental design, the potential effects between Douglas fir and West-Slope pellet fuel cannot be ruled out.

The estimated PM_{10} mass deposited upon each snapwell with air-liquid interfaced cells for each of the three stove models can be observed in Table 3 below.

Stove Model	**Estimated PM_{10} Mass ($\mu g/cm^2$)**
Three Stone Fire	20 - 30
Envirofit G3300	5 - 9
Philips Gasifier	2 – 4
Control (room air)	0

Table 3. The estimated PM_{10} mass delivered to NHBE cells grown at an air-liquid interface and exposed to cook stove emissions within the EAVES chamber. Dose was estimated per unit growth area.

As can be seen in Table 3, the three stone fire was estimated to deliver a PM_{10} mass to the NHBE cells that was two to six times greater than the PM_{10} mass delivered by the Envirofit G3300 Stove and five to fifteen times greater than the PM_{10} mass delivered by the Philips Gasifier. The total PM_{10} mass collected for each of the stoves can be used with the ICRP model for the fractional deposition estimates for PM ranging from 20-1000 nm to estimate the PM_{10} mass deposited in the bronchiole/bronchiolar region of the lungs of a human adult with a resting breathing rate.[32] Assuming a breathing rate of 1.2 m^3 per hour, and nose breathing, a human adult would have deposited 0.015-0.09 $\mu g/cm^2$ if exposed to the three stone fire, 0.003-0.02 $\mu g/cm^2$ if exposed to the G3300, and 0.001-

0.009 μg per cm^2 of bronchiolar lung tissue if exposed to the Gasifier for the duration of 45 minutes at a simmer phase. The PM_{10} mass delivered to the NHBE cells during these experiments was substantially larger (300-2000x greater) than the estimated PM_{10} mass that would be delivered to the bronchial cells of a human exposed to the stove models for the duration of the simmer test (45 minutes). However, in the field, normal human bronchial epithelium would be exposed to the emissions from a wood burning stove for a much longer duration than 45 minutes. With an estimated mucociliary clearance rate of 0.5% per minute for particles deposited in the ciliated airways (Foster et al. 1982), there is likely a chronic accumulation of deposited PM in the ciliated airways of humans residing in homes with biomass burning.[74] Although the PM_{10} mass delivered to the NHBE cells in these experiments was substantially larger than the estimated PM_{10} mass delivered to the bronchiolar region of the lungs of humans in wood burning homes, the increased delivery of PM_{10} mass to the NHBE cells might serve to compensate for the short duration of exposure (45 minutes) of these experiments.

Due to the EAVES subisokinetic sampling conditions, there may have been an underestimation of the true PM_{10} mass delivered to the cells in the EAVES chamber during cook stove exposures. The subisokinetic sampling error in the EAVES chamber would have been as high as a factor of 5 for a 10 μm particle. However, this discrepancy should not have substantially affected the estimated mass of PM_{10} delivered to the NHBE cells during cook stove exposures as very few particles above one micron are emitted from combustion processes.

Although the three stone fire serves to model a "traditional" stove or open fire used for domestic cooking, heating, and light, the three stone fire does not model every

traditional stove or open fire that is burned in a home globally. Despite the limited ability to capture the variation that exists in "traditional" biomass burning practices worldwide, the three stone fire did serve to model what occurs when biomass is burned without the use of an improved cook stove. The three stone fire serves as a useful gauge for assessing the benefits of using a more fuel efficient cook stove.

3.4. Cytotoxicity and Inflammatory Biomarkers

3.4.1. Cytotoxicity

Lactate dehydrogenase (LDH) release was evaluated as a means of addressing concerns regarding cell viability and cytotoxicity after forty-five minutes of incubation in the EAVES chamber at 4 L/min flow. Relative levels of lactate dehydrogenase release are shown in Figure 11 (n=18 for each stove model, at each time point). Although care was taken to maintain cells at a physiological temperature, humidity, and pH during exposures, there is a concern that the process of flowing air at 4 L/min over the cells for forty-five minutes may induce cell death through desiccation. There is also a concern that ozone produced within the exposure chamber may increase cellular stress.

The measured LDH release from the NHBE cells did not differ significantly after a forty-five minute exposure to emissions from the three stove models tested or after exposure to HEPA filtered room air (controls). Cell viability and cytotoxicity was uniformly affected by the emissions from all stove models and controls, with a median LDH release of 15-20% at one and twenty-four hours post exposure.

There were no significant differences in the variation of LDH release due to the random effects from either donor phenotype or burn day when analyzed using a mixed model (α=0.05). The LDH release profile from all three donor phenotypes and from all

six exposure days is shown in Figure 11. The LDH release profile is shown as a box-whisker plot where the box outlines the second quartile (25-50 % of the data distribution) and third quartile (50-75% of the data distribution) for the percent LDH release distribution for each stove. The median percent LDH release is signified by the line that divides the second and third quartiles. Although the median percent LDH release was consistently between 15 and 20% for all cell exposures and for both the one-hour and twenty-four hour timepoints, there was enough variability between each LDH assay to create a range from 10-35% LDH released as observed by the middle two quartiles for all exposed cells as seen in Figure 11 below. This variability was most likely caused by inter-assay variability. For each LDH release assay performed, an LDH maximum was established by treating an unexposed culture well with a lysis buffer. The LDH maximum level from one LDH assay to the next varied one to two-fold. All exposed cells (stove exposed and room-air exposed cells) for each phenotype, burn day, and time point were normalized to the same LDH maximum so there was little intra-assay variability, but the inter-assay variability induced the wide range of percent LDH release as seen in Figure 11.

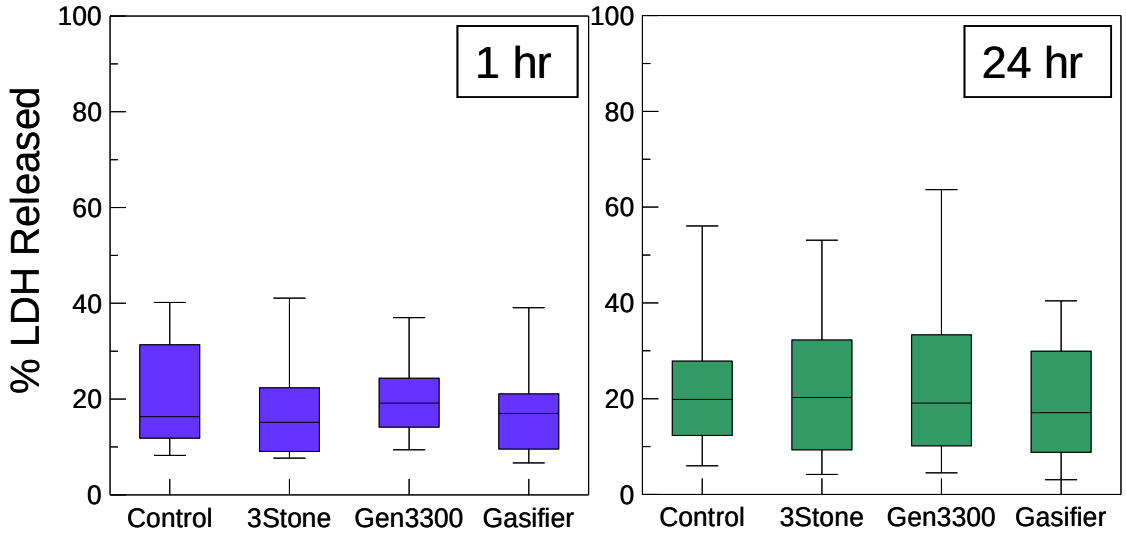

Figure 11. Box-whisker plots of release of lactate dehydrogenase (LDH) from NHBE cells grown at an air-liquid interface at one and twenty-four hours post exposure to cook stove emissions in the EAVES chamber. n=18 for each stove model, at each time point. Controls were exposed to filtered room air.

3.4.2. Inflammatory Biomarkers

The relative expression of inflammatory transcripts by NHBE cells exposed to cook stove emissions is shown in Figure 12. These expression profiles are normalized to both the GAPDH gene[75] and to the expression of mRNA transcripts in the cells exposed to room air (controls).

No significant differences were observed in mRNA expression due to the random effects of either the donor phenotype or burn day. The mRNA transcript expression profile shown in Figure 12 includes data from the three donors and from all six days of cook stove exposures (n=18 for each stove model, at each time point).

The acute cellular response to the three stone fire involved an increased transcription of mRNA coding for Interleukin-8 (IL-8), Heme oxygenase-1 (HOX-1), and Cyclooxygenase-2 (COX-2) proteins. Exposure to emissions from the three stone fire

resulted in cellular accumulations of IL-8, HOX-1, and COX-2 that were significantly elevated above the control cells at one-hour post-exposure (see left side of Figure 12; IL-8, $p=0.02$; HOX-1, $p<0.0001$; COX-2, $p=0.002$). At twenty-four hours post exposure, this same trend was observed, but with reduced statistical significance (see right side of Figure 12; IL-8, $p=0.12$; HOX-1, $p=0.36$; COX-2, $p=0.06$).

The mRNA transcript expression profiles IL-8, HOX-1, and COX-2 at one and twenty-four hours post exposure to emissions from either of the two improved cook stoves was not found to differ significantly from the mRNA transcript expression profiles in cells exposed to room-air. The mRNA transcript expression profiles for each of the three genes of interest are discussed in greater detail below.

Interleukin-8 (IL-8) is a protein involved in the recruitment of neutrophils to sites of inflammation and has recently been implicated to increase blood supply to cells from which it is secreted.[76] At one hour post-exposure the fold change in IL-8 transcription in cells exposed to emissions from the three stone fire was 1.7 (± 0.5), the G3300 was 1.4 (± 0.5), and the Philips Gasifier was 0.9 (± 0.3), relative to the controls. At twenty-four hours post exposure, the mRNA transcript expression levels were similar. The change at twenty-four hours post exposure to the three stone fire was 1.4 (± 0.5), the G3300 was 1.4 (± 0.5), and the Philips Gasifier was 0.8 (± 0.3).

Heme oxygenase-1 is an intracellular enzyme involved in the cellular response to oxidative stress and in mediating oxidative damage in the lung.[77] At one hour post-exposure the fold change in HOX-1 transcription in cells exposed to emissions from the three stone fire was 3.8 (± 1.5), the G3300 was 1.0 (± 0.4), and the Gasifier was 0.8 (± 0.3) (relative to the controls). At twenty-four hours post exposure, the mRNA transcript

expression levels were similar; however, the expression in cells exposed to the 3SF was markedly reduced. The fold change at twenty-four hours post exposure to the 3SF was 1.3 (± 0.5), almost three times less than the level of HOX-1 observed at one hour post exposure. The mRNA transcript levels of HOX-1 observed at twenty-four hours post exposure to either of the improved stoves did not differ significantly from the levels observed at one-hour post exposure.

Cyclooxygenase-2 is a chemokine involved in the prostanoid (pain signaling) pathway and has been indicated to play a role in asthmatic responses of the bronchial epithelium.[78] At one hour post-exposure the fold change in COX-2 transcription in cells exposed to emissions from the three stone fire was 3.0 (± 1.3), the G3300 was 1.0 (± 0.5), and the Gasifier was 0.7 (± 0.3) (relative to the controls). At twenty-four hours post exposure, the mRNA transcript expression levels were similar; however, the mRNA transcript expression in cells exposed to the three stone fire, again, was markedly reduced. The fold change at twenty-four hours post exposure to the three stone fire was 1.8 (± 0.8), almost half the level of COX-2 observed at one hour post exposure. The mRNA transcript levels of COX-2 observed at twenty-four hours post exposure to either of the improved stoves did not differ significantly from the levels observed at one-hour post exposure.

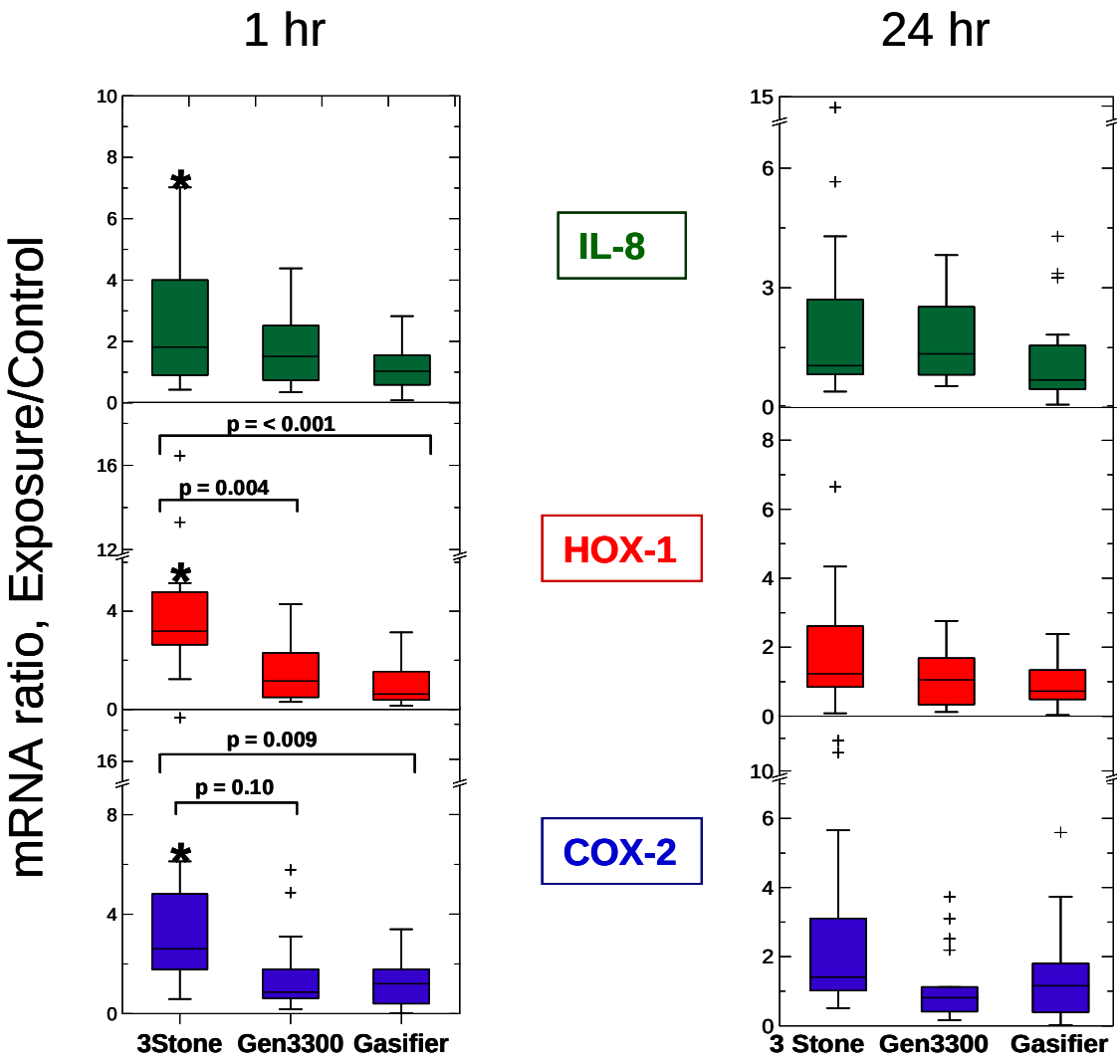

Figure 12. Box-whisker plots of mRNA transcript profiles (ratio of exposure to control) at one-hour (left) and twenty-four hours (right) post-exposure to cook stove emissions (n=18 for each stove model, at each time point). The (+) symbols indicate outliers. The (*) symbols indicate expression profiles that were significantly elevated above the NHBE cells exposed to room air (controls).

3.5. Limitations

A limitation of this study is that only a single cell population (normal, human bronchial epithelial) was studied. Within the body, the increased transcription of IL-8, HOX-1, and COX-2 in NHBE cells might recruit help from other immune cell

populations like macrophages and neutrophils in response to inhaled toxicants. While the in vitro aerosol exposure model used in this study is a closer approximation of human aerosol exposure when compared to conventional human lung epithelial in vitro models, the in vitro model lacks the dynamics involved in the in vivo inflammatory response to include macrophages, neutrophils, a blood supply, smooth muscle structures and innervation.

Another limitation of this study was the small number of human bronchial epithelial phenotypes that were used to evaluate the inflammatory effects of cook stove exhaust. The three donor phenotypes were all healthy, non-smoking individuals who tested negative for H.I.V. and Hepatitis C. The three phenotypes used for this study may not adequately capture the potential inflammatory response of all human bronchial epithelial cells within the human population. Yet, mRNA transcript expression of each inflammatory biomarker was not found to vary significantly between the three phenotypes exposed, which suggests that the cook stove model used to expose the NHBE cells was a more significant predictor in the inflammatory response of the NHBE cells than donor phenotype. Despite the small number of NHBE cell phenotypes tested, there were consistent, significant increases in the mRNA transcript expression of the inflammatory biomarkers of NHBE cells exposed to emissions from the three stone fire, relative controls and the improved cook stoves.

The cellular inflammatory response to biomass combustion aerosol mixtures involves a cascade of cellular responses that results in an increase of enzymes associated with reactive oxygen species scavenging, an increase in cellular antioxidants, and a myriad of cytokines and chemokines responsible for recruiting immune cells to the site of cellular

stress. The cellular production of inflammatory coordinators like TNF-α increase when bronchial epithelial cells are exposed to inhalable oxidants.[53] TNF-α stimulates airway epithelial cells to transcribe genes for pro-inflammatory cytokines and chemokines like IL-8, IL-1, inducible NO synthase, COX-2, ICAM-1, IL-6, MIP-1, GM-CSF, stress response genes like HSP-27, 70, 90, HOX-1, and antioxidant enzymes like glutamylcysteine synthetase, GCS, MnSOD, and thioredoxin.[53] The induction of any one of these genes is associated with inflammation of the human lung. Due to time and cost considerations, only four cellular endpoints were evaluated for this study. However, the selected genes represent a panel of markers that cover the primary modes of cellular insult: immune response, inflammation, and oxidative stress. The analysis of the inflammatory response was also limited to only two timepoints post exposure, which makes it difficult to determine if the peak inflammatory response was captured in our analysis. However, time and cost considerations restricted the analysis of cellular response to one and twenty-four hours post exposure.

4. Conclusions and Future Work

Results from this study indicate that exposure to emissions from an improved cook stove reduces the inflammatory response of normal human bronchial epithelial cells when compared to the cellular response after exposure to emissions from a traditional three stone fire. The most pronounced inflammatory response was observed at one-hour post exposure to emissions from the three stone fire.

Despite the limitations inherent in using an in vitro cell culture approach to model human inhalational exposure, the results from this investigation suggest that the EAVES system can be used with success to model aerosol exposure with NHBE cells grown in vitro at an air-liquid interface. A forty-five minute exposure was sufficient to observe an increased cellular response to emissions without increasing cytotoxicity. The cellular expression profiles for the mRNA transcripts for IL-8, HOX-1, and COX-2 observed in the cells exposed to either of the two improved stoves were not significantly elevated when compared to filtered-air controls. These results do not necessarily indicate that emissions from either of the improved stoves are benign. Rather, the lack of any observed difference between improved cook stove emissions exposure and HEPA-filtered room-air exposure may be an artifact of the duration of cellular exposure. Future work might include longer exposures or higher concentrations such that differences between the improved stove model emissions and room air may be elucidated. However, care must be taken to avoid increased rates of cell death that may be commensurate with increased exposure levels.

The mechanisms associated with the inflammatory response observed in NHBE cells exposed to three stone fire emissions is yet to be fully understood. The SMPS data, gravimetric analysis of the PM_{10} in the emissions, and estimates of the PM_{10} mass delivered to the cells during exposure suggest that the three stone fire produced emissions with particles that were larger in size, mass, and greater in number than the particles emitted from either of the improved stove models. Whether it is wood smoke particle size, mass, or particle number that was most significant in stimulating the increased inflammatory response of NHBE cells after exposure to emissions from the three stone fire remains to be known. Future work might include attempting to elucidate which physical or chemical property of the cook stove combustion emissions best predicts the inflammatory response of human bronchial epithelial cells. Further investigations into the role that aerosol size, mass, surface area, particle shape, redox potential, and gaseous species play in predicting the inflammatory response of human bronchial epithelial cells may help cook stove designers to develop cook stoves that potentially increase human health.

Wood fuel was used in this study but an investigation into the inflammatory potential from the emissions from other biomass fuels (crops like corn husks, coconut skins and shells; dung) is needed. The EAVES exposure system and NHBE cells grown at an air-liquid interface could provide a desirable platform for investigating the effects of fuel type upon the inflammatory response of NHBE cells.

The EAVES chamber could be used in the field provided that a power supply, carbon dioxide, and pumps with mass flow controllers were provided. If no incubator were available, the EAVES chamber could be used to incubate the cells before and after

exposures, but the current system would be limited to nine cell exposure samples. A system that allows for a 96-well plate for cell exposures is currently in development to address this concern, and would provide an appealing improvement to the system described in these experiments as the new system would allow for a higher throughput of cell samples for exposures.

5. References

1. Bruce, Perez-Padilla, and Albalak. Indoor Air Pollution in Developing Countries: A Major Environmental and Public Health Challenge. *Bulletin of the World Health Organization, Special Theme – Environmental Health* **2000**, 78: 1078-1091.

2. Baldwin SF. Biomass Stoves: Engineering Design, Development, and Dissemination. Arlington, VA: *Volunteers in Technical Assistance* **1987**.

3. Goldemberg, Johansson, Reddy, and Williams. A Global Clean Cooking Fuel Initiative. Energy for Sustainable Development **2004**, Vol IIIV, No. 3.

4. Smith, Kirk R. Wood: the Fuel that Warms You Thrice. Human Health and Forests: A Global Overview of Issues, Practice, and Policy. Earthscan, London, **2008**. Chapter 5, pp 97-111.

5. Wallmo, Jacobson. A Social and Environmental Evaluation of Fuel-Efficient Cook-stoves and Conservation in Uganda. Foundation for Environmental Conservation. *Env. Conservation* **1998**, 25(2): 99–108

6. Murray. Lopez. Mortality by Cause for Eight Regions of the World: Global Burden of Disease Study. *The Lancet* **1997**, Vol 349.

7. Naeher, Brauer, Lipsett, Zelikoff, Simpson, Koenig, Smith. Wood Smoke Health Effects: A Review. *Inhalational Toxicology* **2007**, 19: 67-106.

8. Granderson, Sandhu, Vasquez, Ramirez, and Smith. Fuel Use and Design and Analysis of Improved Woodburning Cook Stoves in the Guatemalan Highlands. *Biomass and Bioenergy* **2009**, 33(2): 306-315

9. Photo courtesy of Envirofit International. **2010**.

10. Zhang, Smith, Uma, Ma, Kishore, Khalil, Rasmussen, Thorneloe. Carbon Monoxide from Cook stoves in Developing Countries: 1. Emission Factors. *Chemosphere – Global Change Science* **1999**, 1(1-3): 353-366.

11. OSHA.gov. Occupational and Safety Guidelines for Carbon Monoxide. http://www.osha.gov/SLTC/healthguidelines/carbonmonoxide/recognition.html

12. U.S. EPA. Carbon Monoxide. EPA's Efforts to Reduce Carbon Monoxide. http://www.epa.gov/air/urbanair/co/effrt1.html

13. Dary, Pineda, Belizan. Carbon Monoxide Contamination in Dwellings in Poor Rural Areas of Guatemala. *Bull. Environ. Contam. Toxicol*. **1981**, 26: 24-30

14. Viau, Hakizimana, Bouchard. Indoor Exposure to Polycyclic Aromatic Hydrocarbons and Carbon Monoxide in Traditional Houses in Burundi. *Internat'l Archives of Occup. and Env. Health* **2000**, 73(5):331-338.

15. Bateman DN. Carbon Monoxide. *Medicine* **2003,** 31(10): 233. doi:10.1383/medc.31.10.41.27810.

16. Behera, Dash, Yadav. Carboxyhaemoglobin in women exposed to different cooking fuels. *Thorax* **1991,** 46: 344-346.

17. Behera, Dash, Malik. Blood carboxyhaemoglobin levels following acute exposure to smoke of biomass fuel. *Indian Journal of Medical Research* **1988,** 88: 522-542.

18. U.S. EPA. An Introduction to Indoor Air Quality. Nitrogen Dioxide. http://www.epa.gov/iaq/no2.html#Health%20Effects%20Associated%20with%20Nitrogen%20Dioxide

19. Smith, Samet, Romieu, Bruce. Indoor Air Pollution in Developing Countries and Acute Lower Respiratory Infections in Children. *Thorax* **2000**, 55:518-532 doi:10.1136/thorax.55.6.518

20. World Health Organization. Air Quality and Health. http://www.who.int/mediacentre/factsheets/fs313/en/index.html

21. Kumie, Emmelin, Wahlberg, Berhane, Ali, Mekonnen, Brandstrom. (2008) Magnitude of indoor NO_2 from biomass fuels in rural settings of Ethiopia. *International Journal of Indoor Environment and Health* **2008,** 19(1): 14-21.

22. Kumie, Emmelin, Wahlberg, Berhane, Ali, Mekonnen, Worku, Brandstrom. Sources of variation for indoor nitrogen dioxide in rural residences of Ethiopia. *Environmental Health* **2009,** 8:51.

23. U.S. EPA. Air Toxics. Benzene Fact Sheet. http://www.epa.gov/ttn/atw/hlthef/benzene.html

24. S.N. Sinha et al. Environmental monitoring of benzene and toluene produced in indoor air due to combustion of solid biomass fuels. *Science of the Total Environment* **2006,** 357: 280–287.

25. Bhattacharya M, Sultana S, Hasneen A, Islam S, Sarkar K. Status of volatile organic compounds, suspended particulates matters and lead in ambient air and environments in Dhaka City. BAQ **2002**; Dec, 16–18 Hong Kong SAR, Better Air Quality in Asian and Pacific Rim Cities.

26. Judith T. Zelikoff, Lung Chi Chen, Mitchell D. Cohen, Richard B. Schlesinger. The Toxicology of Inhaled Wood smoke. *Journal of Toxicology and Environmental Health*, Part B **2002**, 5:269–282

27. U.S. EPA. Air Toxics Website. Formaldehyde. http://www.epa.gov/ttn/atw/hlthef/formalde.html

28. Smith, Aggarwal, Dave. Air Pollution and Rural Biomass Fuels in Developing Countries: A Pilot Village Study in India and Implications for Research and Policy. *Atmospheric Environment* **1983,** 17(1 I):2343-2362.

29. Smith, Kirk. Biofuels, Air Pollution, and Health. A Global Review. Plenum Press, New York, NY, **1987**.

30. U.S. EPA Integrated Risk Information System. Napthalene. http://www.epa.gov/iris/subst/0436.htm

31. Hinds. Aerosol Technology. Properties, Behavior, and Measurement of Airborne Particles. Second Edition. John Wiley and Sons Inc, New York, NY, **1999,** pp: 308-310.

32. Task Group of the International Commission on Radiological Protection. Human Respiratory Tract Model for Radiological Protection. ICRP Publication 66, **1994.**

33. Wagner, Krelling, Semmler, Muller. Health Effects of Ultrafine Particles. *Journal of Aerosol Science* **2004,** 35(2):1155-1156.

34. Norboo T et al. Domestic Pollution and Respiratory Illness in a Himalayan Village. *International Journal of Epidemiology* **1991,** 20: 749-57.

35. Opotowsky, Vedanthan, Mamlin. A Case Report of Cor Pulmonale in a Woman Without Exposure to Tobacco Smoke: An Example of the Risks of Indoor Wood Burning. *Medscape J Med*. **2008,** 10(1):22.

36. Anders, Emmelin, Wall. Indoor Air Pollution. A Poverty-Related Cause of Mortality Among the Children of the World. *CHEST* **2007,** 132:1415-1416.

37. World Health Organization. World Health Report 2004: Changing History.

Geneva, Switzerland, **2004.**

38. Smith, Mehta, Maeusezahl-Feuz. Indoor smoke from household solid fuels. Comparative Quantification of Health Risks: Global and Regional Burden of Disease due to Selected Major Risk Factors. World Health Organization. Geneva, Switzerland, **2004,** pp 1435-1493.

39. Smith, Bruce, Arana. RESPIRE: The Guatemala Randomized Trial. *Epidemiology* **2006,** 17(6): S44-46.

40. Barregard, Sallsten, Gustafson, Andersson, Johansson, Stigendal. Experimental Exposure to Wood-smoke Particles in Healthy Humans: Effects on Markers of Inflammation, Coagulation, and Lipid Peroxidation. *Inhalational Toxicology* **2006,** 18: 845-853

41. Barregard, Sallsten, Andersson, Almstrand, Gustafson, Andersson, Oli. Experimental exposure to wood smoke: effects on airway inflammation and oxidative stress. *Occupational and Environmental Medicine* **2008,** 65:319-324.

42. Gurgueira, S.A.; Lawrence, J.; Coull, B.; Murthy, G.G.; Gonzalez-Flecha, B. Rapid Increases in the Steady-state Concentration of Reactive Oxygen Species in the Lungs and Heart after Particulate Air Pollution Inhalation. *Environ. Health Perspective* **2002,** 110: 749-755.

43. Lowry, W.T., Peterson, J., Petty, C.S. and Badgett, J.L. Free Radical Production from Controlled Low-energy Fires: Toxicity Considerations. *J. Forensic Sci.* **1985,** 1**:** 73–85

44. Yamaguchi, K.T., Stewart, R.J., Wang, H.M., Hudson, S.E., Vierra, M., Akhtar, A., Hoffman, C. and George, D. Measurement of Free Radicals from Smoke Inhalation

and Oxygen Exposure by Spin Trapping and ESR Spectroscopy. *Free Rad. Res. Comms.* **1992, (**16**)**3:167–174

45. Stohs, S.J.; Bagchi, D. Oxidative Mechanisms in the Toxicity of Metal Ions. *Free Radical Biology Medicine* **1995,** 18: 321-336.

46. Donaldson, K.; Stone, V. Current Hypotheses on the Mechanisms of Toxicity of Ultrafine Particles. *Ann. 1st. Super. Sanita.* **2003,** 39: 405-410.

47. Christos Hatzis, John Godleski, Beatriz Gonzalez-Flecha, Jack Wolfson, and Petros Koutrakis. Ambient Particulate Matter Exhibits Direct Inhibitory Effects on Oxidative Stress Enzymes. *Env. Science Technology* **2006,** 40: 2805-2811

48. Tjalkens. Toxicants of the Respiratory System. Lecture 10, class notes for EH 502, Fall **2007**.

49. Karlsson, Ljungman, Lindbom, Moller. Comparison of Genotoxic and Inflammatory Effects of Particles Generated by Wood Combustion, a Road Simulator and Collected from Street and Subway. *Toxicological Letters* **2006,** 165:203-211

50. Leonard, Wang, Shi, Jordan, Castranova, Dubick. Wood Smoke Particles Generate Free Radicals and Lipid Peroxidation, DNA Damage, NFkappaB Activation and TNF-alpha Release in Macrophages. *Toxicology* **2000,** 150: 147-157

51. Danielsen, Loft, Kocbach, Schwarze, Moller. Oxidative Damage to DNA and Repair Induced by Norwegian Wood Smoke Particles in Human A549 and THP-1 Cell Lines. *Gen Toxicol Environ Mut.* **2009,** 674:116-122.

52. National Institute for Occupational Safety and Health. RTECS. Benzo(a)pyrene. http://www.cdc.gov/niosh/rtecs/dj381378.html

53. Rahman. Oxidative Stress, Chromatin Remodeling and Gene Transcription in

Inflammation and Chronic Lung Diseases. *Journal of Biochemistry and Molecular Biology* **2003,** 36(1): 95-109.

54. Costa, D. L.; Aufderheide, M.; Devlin, R. B.; Feron, V.; Harkema, J.; Hayashi, Y.; Pauluhn, J.; Spielmann, H. Workshop on Experimental Assessment of the Toxicological Effects of Inhaled Complex Mixtures on the Respiratory System - Feasibility and Limitations: Summary and Conclusions of the Review Committee. *Exp. Toxicol. Pathol*. **2005,** 57 (Suppl. 1), 239.

55. Andrea J. Ross, Lisa A. Dailey, Luisa E. Brighton, Robert B. Devlin. Transcriptional Profiling of Mucociliary Differentiation in Human Airway Epithelial Cells. *American Journal of Respiratory Cell and Molecular Biology* **2007,** 37: 169-185.

56. Volckens, Dailey, Roberts, Devlin. Direct Particle-to-Cell Deposition of Coarse Ambient Particulate Matter Increases the Production of Inflammatory Mediators from Cultured Human Airway Epithelial Cells. *Environment Science and Technology* **2009,** 43: 4595-4599.

57. Aufderheide, M.; Mohr, U. CULTEX--An Alternative Technique for Cultivation and Exposure of Cells of the Respiratory Tract to Airborne Pollutants at the Air/Liquid Interface. *Exp. Toxicol. Pathol.* **2000,** 52(3): 265–270.

58. Cheng, M. D.; Malone, B.; Storey, J. M. (2003) Monitoring cellular responses of engine-emitted particles by using a direct air-cell interface deposition technique. *Chemosphere* **2003,** 53(3): 237–43.

59. de Bruijne, K.; Ebersviller, S.; Sexton, K.; Lake, S.; Leith, D.; Goodman, R.; Jetter, J.; Doyle-Eisele, M.; Walters, G.; Woodside, R.; Jeffries, H.; Jaspers, I. Design and Testing of Electrostatic Aerosol In Vitro Exposure System (EAVES): An Alternative

Exposure System for Particles. *Inhalation Toxicol.* **2009,** 21,:91-101.

60. Bosson, J.; Barath, S.; Pourazar, J.; Behndig, A. F.; Sandstrom, T.; Blomberg, A.; Adelroth, E. Diesel Exhaust Exposure Enhances the Ozone-induced Airway Inflammation in Healthy Humans. *Env. Respir. J.* **2008,** 31(6): 1234–1240.

61. Engines and Energy Conversion Laboratory. Department of Mechanical Engineering. Colorado State University. Fort Collins, CO. http://www.eecl.colostate.edu/

62. Envirofit International. Clean Cook stoves Project. http://www.envirofit.org/?q=our-products/clean-cook stoves

63. Lonza. Shop. Products. NHBE-Normal Human Bronchial/Tracheal Cells, without retinoic acid.

64. Lonza. Shop. Products. BEGM-Bronchial Epithelial Growth Medium. https://bcprd.lonza.com/shop/b2c/display/(xcm=lonza_b2b&layout=5.1-6_1_75_65_8_11&uiarea=2&carea=DCEA1752F95290F18C7C001A4B525E10&cpgnum=1)/.do

65. Photo courtesy of Christian L'Orange. Department of Mechanical Engineering. CSU. Fort Collins, CO 80521

66. EPA Test Method 320, Measurement of Vapor Phase Organic and Inorganic Emissions by Extractive Fourier Transform Infrared Spectroscopy. http://www.epa.gov/ttn/emc/promgate/m-320.pdf

67. Rob Bailis, Damon Ogle, Nordica Macarty, and Dean Still. The Water Boil Test Procedure 3.0. **2007.** http://ehs.sph.berkeley.edu/hem/hem/protocols/WBT_Version_3.0_Jan2007a.pdf

68. R. Subramanian, Andrey Y. Khlystov, Juan C. Cabada, Allen L. Robinson.

Positive and Negative Artifacts in Particulate Organic Carbon Measurements with Denuded and Undenuded Sampler Configurations. *Aerosol Science and Technology* **2004,** 38(12, Suppl. 1):27 – 48.

69. Allan, Rushton. Use of the Cytotox(96) in Routine Biocompatibility testing in vitro. *Promega Notes Magazine* **1994,** 45:7.

70. Evans, MJ, Van Winkle, LS, Fanucchi, MV, Plopper. Cellular and Molecular Characteristics of Basal Cells in Airway Epithelium. *Experimental Lung Research* **2001,** 27:401-415.

71. M Ezzati, H Saleh, and D M Kammen. The contributions of emissions and spatial microenvironments to exposure to indoor air pollution from biomass combustion in Kenya. *Environ Health Perspect* **2000** 108(9): 833–839.

72. World Health Organization. Fuel for Life: Household Energy and Health. WHO Press, Geneva Switzerland, 2006.

73. L'Orange, Christian. Testing Methodologies for Cook Stoves and their Effects on Emissions. M.S. Thesis. Department of Mechanical Engineering, Colorado State University, **2009**.

74. Foster, W.M., Langenback, E.G., Bergofsky, E.H. Lung Mucociliary Function in Man: Interdependence of Bronchial and Tracheal Mucus Transport Velocities with Lung Clearance in Bronchial Asthma and Healthy Subjects. *Ann. occup. Hyg.*, **1982** Vol. 26, No. 2, pp. 227-244

75. Robert D. Barber, Dan W. Harmer, Robert A. Coleman and Brian J. Clark. GAPDH as a Housekeeping Gene: Analysis of GAPDH mRNA Expression in a Panel of 72 Human Tissues. *Physiological Genomics* **2005,** 21:389-395.

76. Schraufstatter, Chung, Berger. The Angiogenic Role of Interleukin-8 in Lung Cancer. *American Journal of Physiology* **2001,** 280: L1094-L1103.

77. Choi AM, Alam J. Heme oxygenase-1: Function, Regulation, and Implication of a Novel Stress-inducible Protein in Oxidant-induced Lung Injury. *American Journal of Resp. Cellular Molecular Biology* **1996,** 15(1): 9-19.

78. Peter E. Lipsky, MD; Peter Brooks, MD; Leslie J. Crofford, MD; Raymond DuBois, MD, PhD; David Graham, MD; Lee S. Simon, MD; Leo B. A. van de Putte, MD, PhD, FRCP; Steven B. Abramson, MD. Unresolved Issues in the Role of Cyclooxygenase-2 in Normal Physiologic Processes and Disease. *Archives of Internal Medicine* **2000,** 160: 913-920.

Appendix A

The nucleotide sequences used to generate the primers used for the real time RT PCR analysis of the mRNA expression profiles for COX-2, HOX-1, IL-8, and GAPDH can be seen below.

Oligo Human	ID	5'-3'	Accession	Base Pairs
COX-2	sense (forward)	GAATCATTCACCAGGCAAATTG	M90100	1325-1346
COX-2	anti-sense	TCTGTACTGCGGGTGGAACA	M90100	1391-1372
HOX-1	sense (forward)	CAGCAACAAAGTGCAAGATTCTG	NM_002133	800-822
HOX-1	anti-sense	AGTGTAAGGACCCATCGGAGAAG	NM_002133	901-879
IL-8	sense (forward)	TTGGCAGCCTTCCTGATTTC	M28130	1611-1630
IL-8	anti-sense	TATGCACTGACATCTAAGTTCTTTAGCA	M28130	2510-2483
GAPDH	sense (forward)	GAAGGTGAAGGTCGGAGTC	M33197	66-84
GAPDH	anti-sense	GAAGATGGTGATGGGATTTC	M33197	291-272